Geochemistry Geophysics Geosystems G3
AN ELECTRONIC JOURNAL OF THE EARTH SCIENCES
Published by AGU and the Geochemical Society

Technical Brief
Volume 10, Number 4
10 April 2009
Q04010, doi:10.1029/2009GC002400
ISSN: 1525-2027

Click Here for Full Article

Precise determination of Phanerozoic zircon Pb/Pb age by multicollector SIMS without external standardization

Xian-Hua Li, Yu Liu, Qiu-Li Li, and Chun-Hua Guo
State Key Laboratory of Lithospheric Evolution, Institute of Geology and Geophysics, Chinese Academy of Sciences, Beijing 100029, China (lixh@gig.ac.cn)

Kevin R. Chamberlain
Department of Geology and Geophysics, University of Wyoming, Laramie, Wyoming 82071, USA

[1] Zircon has long been recognized as the best geochronometer and the most important timekeeper in geosciences. Modern microbeam techniques such as SIMS and LA-ICPMS have been successfully applied to in situ U-Pb zircon age determinations, at spatial resolutions of 20–30 μm or less. Matrix-matched calibration by external standardization of well-characterized natural zircon references is a principal requirement for precise microbeam U-Pb zircon age determination due to fractionation effects between Pb and U, which usually result in an external age error exceeding 1%. Alternatively, zircons with a closed U-Pb system can be directly dated by measurement of ^{207}Pb/^{206}Pb isotopic ratio without external standardization, which has been a common practice for zircons older than 1.0 Ga, but not for relatively young (<1.0 Ga and particularly Phanerozoic) ones because of limitations of analytical precision. We describe in this paper a method of ^{207}Pb/^{206}Pb measurement on Phanerozoic zircons using a new generation of large radius magnetic sector multicollector Cameca IMS-1280 SIMS. In combination with multicollector mode, a Nuclear Magnetic Resonance (NMR) magnet controller and oxygen flooding techniques, we achieve precisions of ^{207}Pb/^{206}Pb ratio of <0.1% and 0.1 $\sim$ 0.2%, propagating to Pb/Pb age errors <0.4% and 1–3% (excluding U decay constant uncertainties), for zircons of latest Neoproterozoic and late Paleozoic to Mesozoic age, respectively. Therefore, the multicollector SIMS is capable of direct determination of zircon Pb/Pb ages as young as Mesozoic age with uncertainties of geological significance. This technique is useful for direct dating of zircons in thin sections. Moreover, it has significance for dating of some other U-rich minerals (i.e., baddeleyite and zirconolite) that are not suitable for SIMS U-Pb dating by external standardization.

Components: 11,406 words, 12 figures, 4 tables.

Keywords: SIMS; multicollector; zircon; Pb/Pb age; Phanerozoic.

Index Terms: 1194 Geochronology: Instruments and techniques; 1115 Geochronology: Radioisotope geochronology.

Received 26 January 2009; **Accepted** 2 March 2009; **Published** 10 April 2009.

Li, X.-H., Y. Liu, Q.-L. Li, C.-H. Guo, and K. R. Chamberlain (2009), Precise determination of Phanerozoic zircon Pb/Pb age by multicollector SIMS without external standardization, *Geochem. Geophys. Geosyst.*, *10*, Q04010, doi:10.1029/2009GC002400.

1. Introduction

[2] Zircon, $ZrSiO_4$, is a common U-rich accessory mineral occurring in a wide range of rocks, and has long been recognized as the best geochronometer based on the radioactive decay of U to Pb and the most important timekeeper in geosciences. U-Pb zircon dating techniques achieve great advancements during the past half century [e.g., *Davis et al.*, 2003]. Among them, recent developments in microbeam analysis using SIMS (secondary ion mass spectrometer) and laser ablation (LA)-ICPMS have been widely, successfully applied in U-Pb zircon geochronology [e.g., *Ireland and Williams*, 2003; *Košler and Sylvester*, 2003; *Yuan et al.*, 2008].

[3] It is well known that significant fractionation effect between Pb and U is a major problem with U-Pb zircon age determination using microbeam techniques. The principle strategy to overcome this effect is matrix-matched calibration by analysis of well-characterized natural zircon standards. Thus, precision and accuracy of U-Pb zircon age data are highly controlled by the characterization (particularly homogeneity and concordance) of radiogenic Pb/U ratios of the zircon standards. Despite great efforts of development of natural zircon standards for many years in geoscience community, the ideal zircon U-Pb age standards are still rare. For instance, the SL13 zircon, a gem quality mineral from Sri Lanka with an assigned age of 572 Ma, has long been used a standard for SHRIMP U-Pb zircon age determination. However, it has been recognized that SL13 has a bimodal distribution of $^{206}Pb/^{238}U$ ages: an original crystallization at 580 Ma and Pb loss at 565 Ma [*Compston*, 1999]. In general, with present Pb/U calibration techniques, the precision of SIMS determinations of $^{206}Pb/^{238}U$ appears limited to about 1% [*Ireland and Williams*, 2003].

[4] ^{238}U and ^{235}U decay respectively to produce ^{206}Pb and ^{207}Pb at different rates (half-life of ^{238}U and ^{235}U are 4468 Ma and 704 Ma, respectively), thus the $^{207}Pb/^{206}Pb$ isotope ratio provides a direct measure of age that is independent of Pb/U measurement. In other words, there is a clear advantage for microbeam Pb/Pb age measurement over U/Pb in a closed U-Pb system, because Pb/U calibrations of standard, which usually has 1% or larger uncertainties, is not necessary. In fact, direct measurement of Pb/Pb age by SIMS is a common practice for zircons and other U-rich minerals older than 1.0 Ga, but not for the relatively young (<1.0 Ga and particularly Phanerozoic) samples because of limitations of analytical precision.

[5] We developed in this study a new method of $^{207}Pb/^{206}Pb$ measurements on young (Phanerozoic) zircons using a large radius magnetic sector multicollector Cameca IMS-1280 SIMS, with aims of achieving $^{207}Pb/^{206}Pb$ analytical precision of $\sim$0.2% or better for Phanerozoic (late Paleozoic and Mesozoic) zircons. Our results indicate that the multicollector SIMS is able to determine zircon Pb/Pb ages as young as the Mesozoic age with uncertainties of within a few million years that are of geological significance.

2. Error Propagations of Radiogenic $^{207}Pb/^{206}Pb$ Age Measurements

[6] Despite the aforementioned advantage of SIMS Pb/Pb zircon age measurement, there is also a disadvantage in SIMS $^{207}Pb/^{206}Pb$ age measurement for young (<1.0 Ga and particularly Phanerozoic) samples due to the following reasons. (1) ^{235}U comprises <1% in natural U and so little radiogenic ^{207}Pb is produced in the Phanerozoic that it is difficult to be measured in situ with high precision; (2) the change in radiogenic $^{207}Pb/^{206}Pb$ for Phanerozoic samples is small, varying from 0.058 to 0.046 between 540 Ma and present day; (3) radiogenic $^{207}Pb/^{206}Pb$ measurement is very sensitive to the common Pb correction; and (4) there are significant error magnifications for Phanerozoic Pb/Pb age measurements.

[7] Figure 1 illustrates the error propagations of $^{207}Pb/^{206}Pb$ age measurements. It is clearly shown that uncertainties of radiogenic $^{207}Pb/^{206}Pb$ measurements propagate small errors in early Precambrian samples, but significantly magnified errors in Phanerozoic ones. For example, a 1% error of radiogenic $^{207}Pb/^{206}Pb$ measurement in 3200 Ma, 1600 Ma, 800 Ma, 400 Ma, 200 Ma and 100 Ma old samples results in 0.5%, 1.2%, 2.7% 5.7%, 11.7% and 23% errors in the calculated ages, respectively. Therefore, radiogenic $^{207}Pb/^{206}Pb$ measurements with precisions of $\sim$0.2% are minimum requirements for dating Paleozoic and Mesozoic crystals with age uncertainties of geological significance. This precision requirement is still not as good as that of routine measurement by ID-TIMS that usually gives precision better than 0.1% for $^{207}Pb/^{206}Pb$ measurement, but it has never been achieved in previous in situ SIMS measurements.

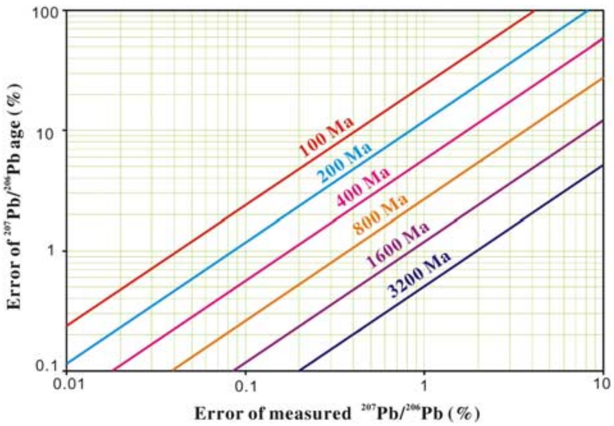

Figure 1. Error propagation between radiogenic $^{207}Pb/^{206}Pb$ ratio and $^{207}Pb/^{206}Pb$ age.

[8] It is noteworthy that uncertainties in the uranium decay constants (0.14% for ^{235}U and 0.11% for ^{238}U [*Jaffey et al.*, 1971]) are an important source of external error in U-Pb and Pb/Pb zircon geochronology [e.g., *Schoene et al.*, 2006] regardless of the dating techniques. To present data at each level of error propagation, the calculated U-Pb and Pb/Pb age errors in this study are reported in the manner of ±X/Y at 95% confidence interval, unless otherwise noted, where X is the internal error including standard calibration (for U-Pb age) and common lead correction but ignoring the decay constant error(s), and Y includes the decay constant error(s) of *Jaffey et al.* [1971]. The algorithms of *Ludwig* [1980] and the statistical reduction and plotting program Isoplot/Ex [*Ludwig*, 2001] were used to calculate ages, uncertainties, weighted means, and the generation of U-Pb concordia plots.

3. Strategy of Improving Precision of Radiogenic $^{207}Pb/^{206}Pb$ Measurement

[9] Increase of the counting time on ^{207}Pb can improve the precision of $^{207}Pb/^{206}Pb$ measurements to some extent, but there are practical limits as it increases risk of partial signal loss due to instrumental drift in monocollector SIMS [e.g., *Ireland and Williams*, 2003]. In addition, signal variation also hampers the improvement of analytical precision by using monocollector SIMS. In fact, it is very rare to achieve precision of better than 0.5% for $^{207}Pb/^{206}Pb$ measurements of Phanerozoic zircons by using monocollector SIMS, as evidenced by large numbers of zircon age data determined by SHRIMP and Cameca SIMS in the literature.

[10] The precision of $^{207}Pb/^{206}Pb$ measurements could be significantly improved by using a new generation multicollector SIMS such as the Cameca IMS-1280 SIMS. Simultaneous detection of ^{206}Pb and ^{207}Pb signals using multicollector mode can eliminate the effect of signal variation. In addition, this new generation SIMS is equipped with an NMR magnet controller that consists of a set of NMR probe and associated electronics. The NMR control, which is used in multicollector mode when no mass peak switching is required, provides a much better stability of magnetic field than the Hall probe system.

[11] Oxygen flooding is another very useful technique in the Cameca SIMS to improve the precision of $^{207}Pb/^{206}Pb$ measurements. Previous investigations demonstrated that introduction of oxygen into the sample chamber (oxygen flooding) of the Cameca SIMS increase the secondary ion yield by ~200% for zircon analysis [e.g., *Schuhmacher et al.*, 1994; *Quidelleur et al.*, 1997; *Whitehouse et al.*, 1999]. Whereas, the Pb^+ ion yield increases only by ~20% under the same oxygen flooding conditions for SHRIMP [*Ireland and Williams*, 2003].

[12] It is anticipated that $^{207}Pb/^{206}Pb$ measurements with precisions of ~0.2% or better might be achieved for Phanerozoic zircons by using the new generation large geometry Cameca IMS-1280 SIMS in combination with multicollector mode, an NMR magnet controller and oxygen flooding techniques.

4. Analytical Procedures

[13] Pb/Pb and U/Pb dating of zircon was conducted using the Chinese Academy of Sciences Cameca IMS-1280 ion microprobe (CASIMS) at the Institute of Geology and Geophysics in Beijing. We use the monocollector mode to determine zircon Pb/Pb and U/Pb ages, and use the multicollector mode to determine zircon Pb/Pb ages only.

[14] U-Pb ID-TIMS dating of the Qinghu zircon was performed at the University of Wyoming, USA, using a modified chemical abrasion method after *Mattinson* [2005] and a Micromass Sector 54 thermal ionization mass spectrometer.

4.1. Monocollector Mode

[15] The O_2^- primary ion beam was accelerated at −13 kV, with an intensity of ~10 nA. The aperture illumination mode (Kohler illumination) was used

with a 200 μm primary beam mass filter (PBMF) aperture to produce even sputtering over the entire analyzed area. The ellipsoidal spot is about 20 × 30 μm in size. Positive secondary ions were extracted with a 10 kV potential.

[16] Oxygen flooding was used to increase the O_2 pressure to ~5 × 10^{-6} Torr in the sample chamber, enhancing Pb^+ sensitivity to a value of 25–28 cps/nA/ppm for zircon. This great enhancement of Pb^+ sensitivity is crucial to improve precision of $^{207}Pb/^{206}Pb$ zircon measurement.

[17] In the secondary ion beam optics, a 60 eV energy window was used, together with a mass resolution of ~5400 (defined at 10% peak height) to separate Pb^+ peaks from isobaric interferences. Precise mass calibration was kept by using an automatic routine in the Cameca Customisable Ion Probe Software (CIPS) to scan over large peaks such as $^{94}Zr_2^{16}O$ and $^{177}Hf^{16}O_2$ and extrapolate the mass to B field curve for peaks between these reference points. The field aperture was set to 7000 μm, and the transfer optic magnification was adjusted to 200. Rectangular lenses were activated in the secondary ion optics to increase the transmission at high mass resolution. A single electron multiplier was used on ion-counting mode to measure secondary ion beam intensities by peak jumping sequence: 196 ($^{90}Zr_2^{16}O$, matrix reference for centering the secondary ion beam as well as energy and mass adjustment), 200 ($^{92}Zr_2^{16}O$, reference of mass 200.5), 200.5 (background), 203.81 ($^{94}Zr_2^{16}O$, for mass calibration), 203.97 (Pb), 206 (Pb), 207 (Pb), 208 (Pb), 209 ($^{177}Hf^{16}O_2$, for mass calibration), 238 (U), 248 ($^{232}Th^{16}O$), 270 ($^{238}U^{16}O_2$), and 270.1 (reference mass), 1.04, 0.56, 4.16, 0.56, 6.24, 4.16, 6.24, 2.08, 1.04, 2.08, 2.08, 2.08, and 0.24 s (the integration time is based on the unit time of 0.08 s), respectively. Each measurement consists of 10 cycles, and the total analytical time is ~16 min.

[18] zzzzzzCalibration of Pb/U ratios is based on an observed linear relationship between $\ln(^{206}Pb/^{238}U)$ and $\ln(^{238}U^{16}O_2/^{238}U)$, as same as those reported by *Whitehouse et al.* [1997]. The relationship between $^{206}Pb/^{238}U$ and $^{238}U^{16}O_2/^{238}U$ can be approximated over a wide range of $^{238}U^{16}O_2/^{238}U$ by a power law relationship. Since the range of measured $^{238}U^{16}O_2/^{238}U$ ratios is small in both standard and unknowns during a particular analytical session, a linear function is chosen to approximate this relationship, with a slope of the $\ln(^{206}Pb/^{238}U)$ – $\ln(^{238}U^{16}O_2/^{238}U)$ calibration line being 1.3. Pb/U calibration was performed relative to the 1065 Ma standard zircon 91500 with Th and U concentrations of ~29 and 80 ppm respectively [*Wiedenbeck et al.*, 1995]. U and Th concentration determination of unknowns is based on observed correlation between $^{238}U^{16}O_2$, $^{232}Th^{16}O$ and $^{90}Zr_2^{16}O$ for the standard. It is noteworthy that this determination of U and Th is considered approximate because of ~15% heterogeneity in U and Th contents for 91500 [*Wiedenbeck et al.*, 2004].

4.2. Multicollector Mode

[19] The multicollector assembly fitted to this large geometry Cameca IMS-1280 SIMS instrument consists of five movable trolleys, each of which may be equipped with either electron multiplier (EM) or Faraday cup (FC). Figure 2 shows the multicollector configuration for Pb/Pb dating of zircon.

[20] In the secondary ion beam optics, a 60 eV energy window was used throughout, together with a mass resolution of ~4800 (defined at 50% peak height), as the mass resolution is fixed at 2500, 4800 and 8000 in multicollector mode in the Cameca IMS-1280 SIMS. This mass resolution, equivalent to mass resolution of ~4000 defined at 10% peak height, is capable of effective separation of the main interferences of molecules of Zr, Hf, Si and O, such as Zr_2O (requiring a mass resolution of ~1200) and HfSi (requiring ~3700). While it is generally thought that to resolve HREE dioxides such as YbO_2 requires a resolution of ~5100 [e.g., *Ireland and Williams*, 2003], *Bosch et al.* [2002] demonstrated YbO_2 can be readily separated at ~3500. Our SIMS analyses in this study indicated that the measured $^{206}Pb/^{204}Pb$ ratios of two standard zircons (BR266 and Plešovice) by multicollector mode at a resolution of ~4000 are comparable with those by single-collector mode at a resolution of ~5400, suggesting that YbO_2 has negligible interference with the Pb isotope measurements at resolution of ~4000. The multicollection mode was used to measure secondary ion beam intensities of ^{204}Pb, ^{206}Pb and ^{207}Pb, with integration times of 6 s. After a 180-s presputtering with 20 μm raster, the energy calibrations were checked by scanning sample HV (from −20 to >80 eV, 4 eV step, 5 eV gap) on mass ^{206}Pb, beam centering control using ^{206}Pb by scanning deflector for field aperture (DTFA) X/Y (500 dig.) and deflector for contrast aperture (DTCA) X (900 dig.). The NMR controller was used in multicollector measurement to stabilize the magnetic field, with an instrumental drift ($\Delta M/M$) less than 2.5 ppm over 16 h (Figure 3). Each

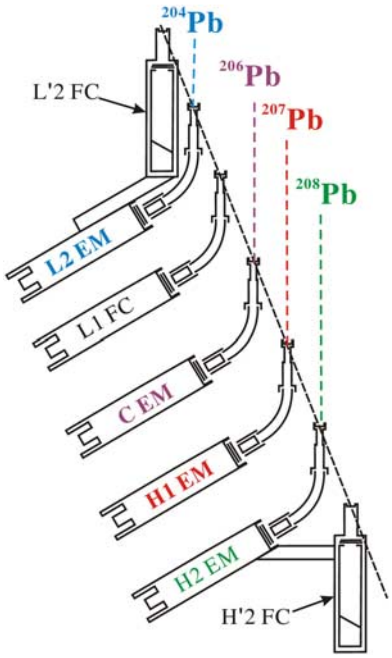

Figure 2. Multicollector configuration for zircon ^{204}Pb, ^{206}Pb, and ^{207}Pb measurement.

measurement consists of 40 cycles, and the total analytical time is ~10 min.

4.3. Correction of Common Pb

[21] Correction of common Pb was made by measuring ^{204}Pb amount. ^{204}Pb provides the direct measure of common Pb, though its low abundance makes the correction relatively imprecise. Accurate peak positioning for ^{204}Pb is crucial for proper estimation of common Pb. In monocollector mode, ^{204}Pb isotope was calibrated by centering the $^{94}Zr_2^{16}O$ peak at nominal mass 204, and then a +0.167 amu mass offset was applied to ^{204}Pb (Figure 4a). In multicollector mode, a high-uranium zircon containing high ^{204}Pb was used to calibrate the Pb peaks (Figure 4b). An average of the isotopic compositions of Pb blank (^{206}Pb/^{204}Pb = 17.8, ^{207}Pb/^{204}Pb = 15.5, ^{207}Pb/^{206}Pb = 0.87) in Beijing TIMS laboratories is used for the common Pb assuming that the low levels of common Pb are thought to be largely laboratory-derived. Because our measured zircon ^{206}Pb/^{204}Pb ratios in this study are mostly higher than 10,000, the common Pb corrections and the calculated U-Pb ages were insensitive to the choice of common Pb isotopic compositions. The high ^{206}Pb/^{204}Pb ratios measured by SIMS in this study are consistent with low-blank TIMS measurements on the same standards [e.g., *Stern and Amelin*, 2003; *Sláma et al.*, 2008] (see also Table 4), which demonstrate that these gem-quality standard zircons are relatively free of initial Pb.

[22] In the multicollector mode analysis, the unradiogenic ^{206}Pb and ^{207}Pb, which were calculated on the basis of the average of measured ^{204}Pb of 40 analytical cycles, were subtracted from the measured ^{206}Pb and ^{207}Pb. Because the average of measured ^{204}Pb counts of 40 analytical cycles gives more precise (~10–30%) and reasonable estimate of the common Pb than that of each cycle, correction of common Pb will contribute a very small error source to the final radiogenic ^{207}Pb/^{206}Pb results when the measured ^{206}Pb/^{204}Pb values are higher than 10,000 (see detailed discussion below).

4.4. Impact of Common Pb Correction on the Age Uncertainty

[23] It is noteworthy that radiogenic ^{207}Pb/^{206}Pb measurement is sensitive to the common Pb correction. We evaluate below quantitatively the impact of common Pb correction on the ^{207}Pb/^{206}Pb age uncertainty.

[24] The radiogenic (^{207}Pb/^{206}Pb)* ratio can be calculated using the following equation:

$$\left(\frac{^{207}Pb}{^{206}Pb}\right)^* = \frac{\left(\frac{^{207}Pb}{^{206}Pb}\right)_m - \left(\frac{^{207}Pb}{^{206}Pb}\right)_c \times f_{206}}{1 - f_{206}} = \frac{\left(\frac{^{207}Pb}{^{206}Pb}\right)_m - \left(\frac{^{207}Pb}{^{206}Pb}\right)_c \times \left(\frac{^{206}Pb}{^{204}Pb}\right)_c \times \left(\frac{^{204}Pb}{^{206}Pb}\right)_m}{1 - \left(\frac{^{206}Pb}{^{204}Pb}\right)_c \times \left(\frac{^{204}Pb}{^{206}Pb}\right)_m} \quad (1)$$

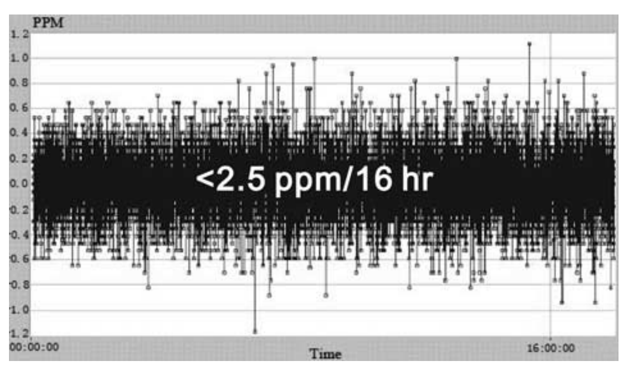

Figure 3. Variations of magnetic field controlled by the NMR controller, which provides a long-term magnetic field drift (ΔM/M) within 2.5 ppm in 16 h. The time interval between field measurements is 1 s, and the integration time for each measurement is 1 s.

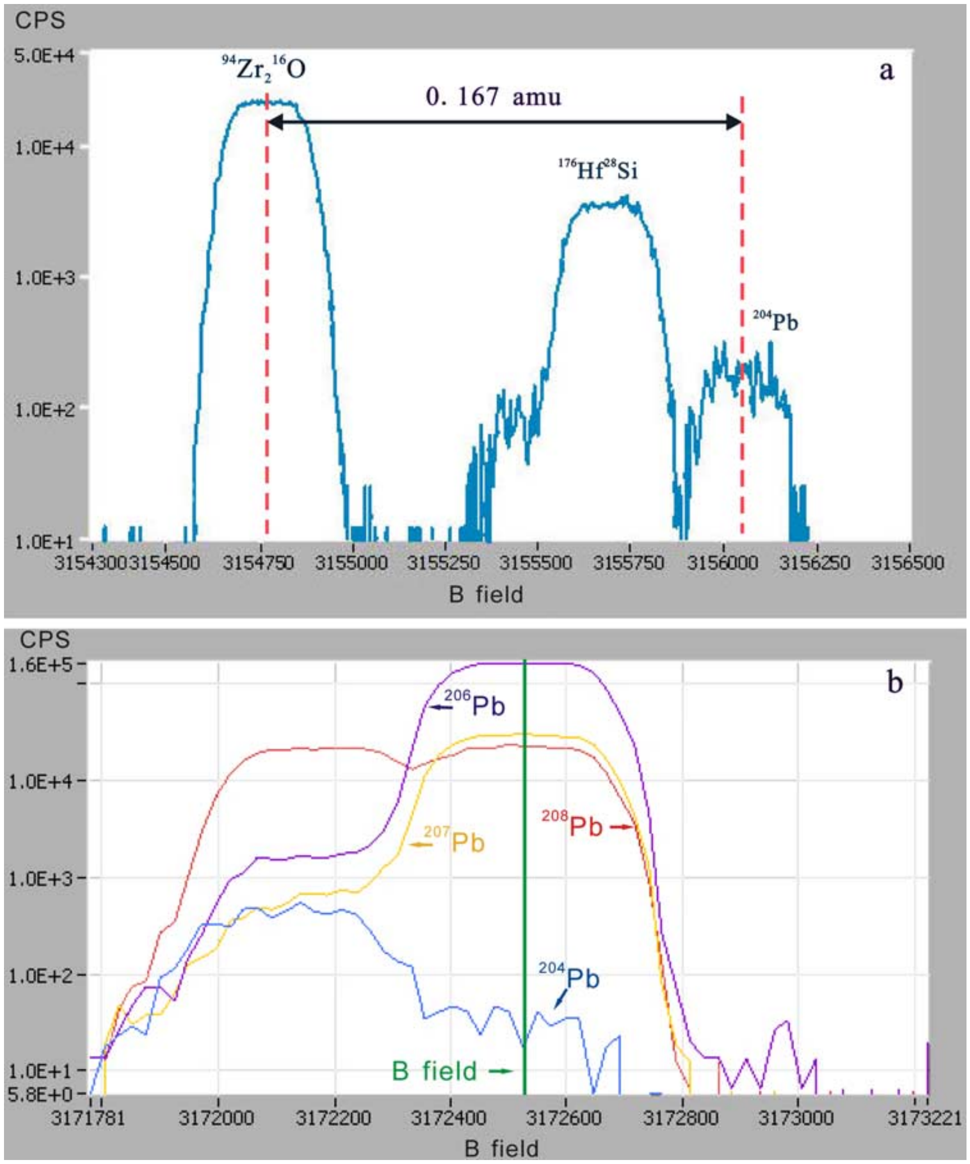

Figure 4. (a) Mass scan of zircon in the region close to mass 204 showing $^{94}Zr_2{}^{16}O$, $^{176}Hf^{28}Si$, and ^{204}Pb peaks at a mass resolution of ∼5400. ^{204}Pb isotope was calibrated by centering the $^{94}Zr_2{}^{16}O$ peak, then adding a +0.167 amu mass offset. (b) Pb mass scan of a high-uranium zircon in Cameca IMS-1280 multicollector array at a mass resolution of ∼4000 (defined at 10% peak height), with more than one third of the peak width being flat at the 99% level.

where c = the common Pb composition; m = the measured value, and f_{206} is the percentage of common ^{206}Pb in total ^{206}Pb, calculated as:

$$f_{206} = \left(\frac{^{206}Pb}{^{204}Pb}\right)_c \times \left(\frac{^{204}Pb}{^{206}Pb}\right)_m \quad (2)$$

[25] Uncertainty of $(^{207}Pb/^{206}Pb)^*$ (σ_z) can be propagated using the following equation:

$$\sigma_z = \sqrt{\left(\frac{\partial Z}{\partial A}\right)^2 * \sigma_A^2 + \left(\frac{\partial Z}{\partial B}\right)^2 * \sigma_B^2 + \left(\frac{\partial Z}{\partial C}\right)^2 * \sigma_C^2 + \left(\frac{\partial Z}{\partial D}\right)^2 * \sigma_D^2} \quad (3)$$

where Z refers to $(^{207}Pb/^{206}Pb)^*$, and A, B, C and D to $(^{207}Pb/^{206}Pb)_m$, $(^{204}Pb/^{206}Pb)_m$, $(^{206}Pb/^{204}Pb)_c$ and $(^{207}Pb/^{206}Pb)_c$, respectively. In equation (3), each differential term (∂) reflects the partial differential of function Z with respect to one variable, holding all others constant. The partial differentials are then multiplied by the absolute (not relative) uncertainties for each variable. The uncertainty on Z is equal to the square root of the sum of the squares of all these terms.

[26] Variations of common Pb compositions are estimated as $^{206}Pb/^{204}Pb$ = 17.6 ± 1, and

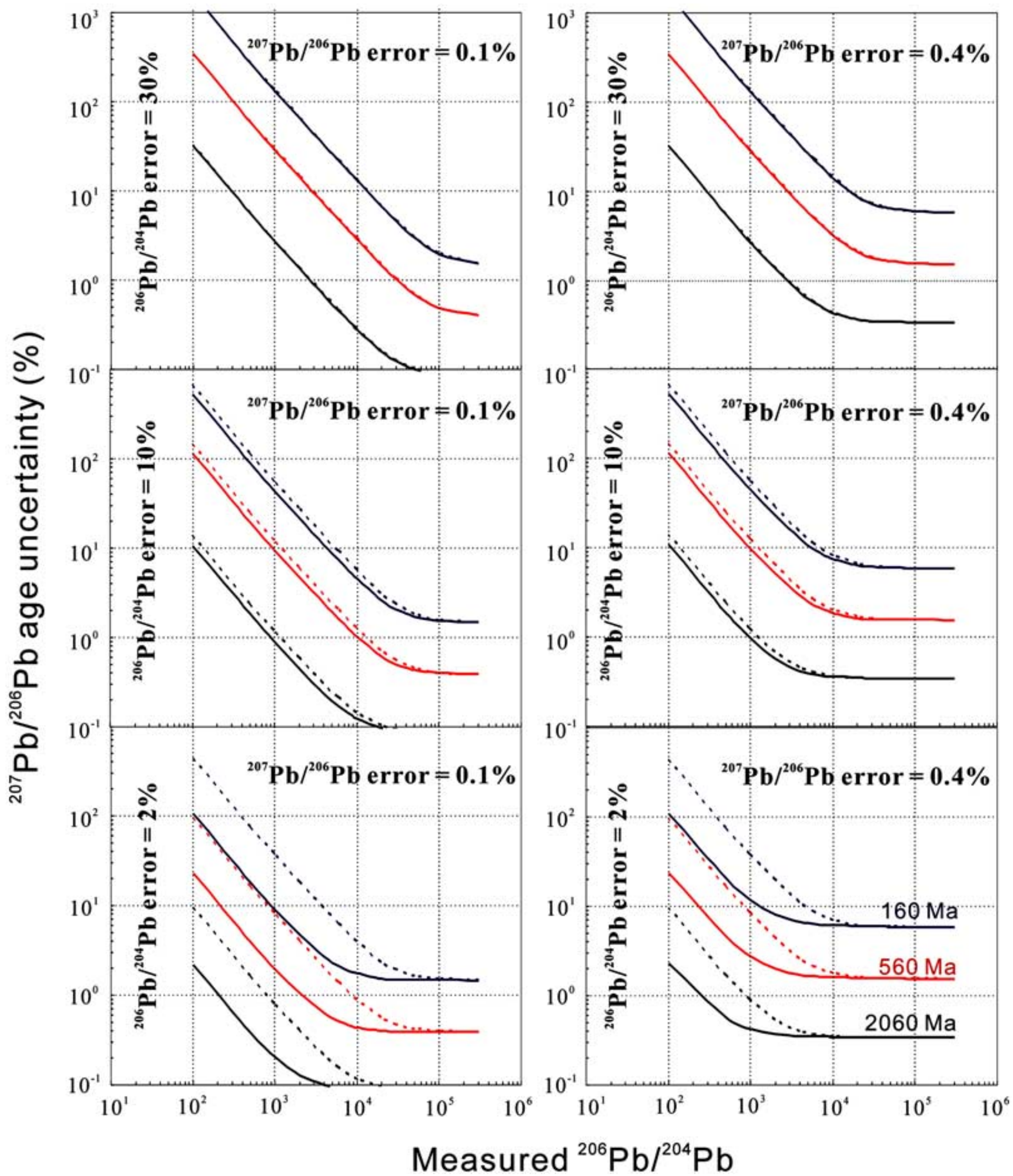

Figure 5. Correlation between uncertainties of the radiogenic $^{207}Pb/^{206}Pb$ ages of 2060 Ma, 560 Ma, and 160 Ma and the measured $^{206}Pb/^{204}Pb$ values, along with assigned uncertainties of measured $^{207}Pb/^{206}Pb$ and $^{206}Pb/^{204}Pb$. Dashed lines include uncertainties of common Pb compositions ($^{206}Pb/^{204}Pb = 17.6 \pm 1$, $^{207}Pb/^{206}Pb = 0.87 \pm 0.05$); solid lines exclude uncertainties of common Pb compositions. SIMS measurements in this study have errors of $^{207}Pb/^{206}Pb$ and $^{206}Pb/^{204}Pb$ mostly ranging from 0.1% to 0.8% and 10% to 30%, respectively, By comparison, TIMS measurements usually have errors of $^{207}Pb/^{206}Pb$ and $^{206}Pb/^{204}Pb$ <0.1% and <2%, respectively. For SIMS measurements, common Pb correction has only little effect on the final Pb/Pb age uncertainty when the measured $^{206}Pb/^{204}Pb > 10,000$.

Table 1. SIMS Baddeleyite Pb/Pb Data

Sample Spot	$^{206}Pb/^{204}Pb_m$[a]	±1σ (%)	$^{207}Pb/^{206}Pb_m$[a]	±1σ (%)	$^{207}Pb/^{206}Pb_c$[b]	±1σ (%)	$t_{207/206}$ (Ma)	±1σ	^{207}Pb (cps)
Monocollector mode									
Phala_s@1	2.40E+05	28.6	0.1268	0.264	0.1268	0.265	2053.9	4.7	6267
Phala_s@2	4.06E+05	36.2	0.1269	0.256	0.1269	0.256	2055.2	4.5	7099
Phala_s@3	3.00E+05	31.1	0.1278	0.346	0.1278	0.346	2067.7	6.1	6692
Phala_s@4	3.43E+05	39.8	0.1276	0.319	0.1276	0.319	2064.8	5.6	4139
Phala_s@5	3.44E+05	40.4	0.1275	0.290	0.1275	0.290	2063.1	5.1	4245
Phala_s@6	2.54E+05	27.5	0.1275	0.295	0.1274	0.296	2062.9	5.2	5356
Phala_s@7	4.04E+05	35.0	0.1275	0.259	0.1275	0.259	2063.2	4.6	5156
Phala_s@8	2.86E+05	31.0	0.1273	0.267	0.1272	0.268	2060.1	4.7	4964
Phala_s@9	3.54E+05	32.7	0.1271	0.277	0.1271	0.277	2058.2	4.9	4628
Phala_s@10	2.32E+05	33.0	0.1269	0.319	0.1269	0.320	2055.1	5.6	4224
Phala_s@11	2.41E+05	33.0	0.1273	0.311	0.1272	0.312	2060.0	5.5	3694
Phala_s@12	4.78E+05	35.0	0.1274	0.238	0.1274	0.238	2061.9	4.2	6195
Phala_s@13	1.51E+05	28.1	0.1268	0.368	0.1267	0.369	2052.5	6.5	3252
Phala_s@14	4.57E+05	40.9	0.1264	0.289	0.1264	0.289	2047.8	5.1	5931
Phala_s@15	1.86E+05	25.0	0.1270	0.237	0.1270	0.237	2056.3	4.2	6448
Phala_s@16	2.71E+05	29.8	0.1267	0.242	0.1267	0.242	2052.6	4.3	6063
Phala_s@17	1.72E+05	25.5	0.1263	0.349	0.1262	0.350	2045.7	6.2	6225
Phala_s@18	1.69E+05	29.8	0.1266	0.306	0.1266	0.307	2050.8	5.4	3777
Phala_s@19	2.84E+05	32.0	0.1275	0.298	0.1275	0.299	2063.4	5.3	3997
Multicollector mode									
Phala_m@1r	5.94E+05	29.3	0.1274	0.126	0.1273	0.126	2061.3	2.2	2960
Phala_m@2r	9.12E+05	38.0	0.1274	0.128	0.1274	0.128	2062.3	2.3	2875
Phala_m@3r	8.56E+05	34.7	0.1271	0.124	0.1271	0.124	2058.2	2.2	3059
Phala_m@4r	3.70E+05	25.6	0.1271	0.146	0.1271	0.147	2058.0	2.6	2198
Phala_m@5r	6.14E+05	26.5	0.1274	0.117	0.1274	0.117	2062.8	2.1	3452
Phala_m@6r	4.62E+05	31.9	0.1273	0.175	0.1273	0.176	2060.4	3.1	1889
Phala_m@7r	3.59E+05	20.7	0.1271	0.126	0.1271	0.126	2057.9	2.2	2975
Phala_m@8r	3.10E+05	27.5	0.1272	0.165	0.1272	0.165	2059.8	2.9	1733
Phala_m@9r	3.80E+05	27.5	0.1272	0.156	0.1272	0.126	2059.7	2.2	1991
Phala_m@10r	3.89E+05	24.1	0.1272	0.133	0.1272	0.134	2059.3	2.4	2648
Phala_m@11r	7.63E+05	38.0	0.1276	0.140	0.1276	0.140	2064.9	2.5	2407
Phala_m@12r	3.46E+05	24.8	0.1270	0.150	0.1270	0.150	2056.8	2.6	2172
Phala_m@13r	1.59E+05	19.9	0.1273	0.154	0.1273	0.155	2060.5	2.7	1987
Phala_m@14r	2.48E+05	20.7	0.1274	0.159	0.1274	0.160	2062.2	2.8	2065
Phala_m@15r	4.00E+05	20.7	0.1273	0.122	0.1272	0.122	2060.0	2.2	3444
Phala_m@16r	3.50E+05	21.7	0.1275	0.127	0.1274	0.127	2063.0	2.2	2943
Phala_m@17r	4.85E+05	24.1	0.1275	0.122	0.1275	0.123	2064.3	2.2	3140
Phala_m@18r	7.37E+05	27.5	0.1272	0.110	0.1272	0.110	2059.5	1.9	3869
Phala_m@19r	4.29E+05	24.8	0.1272	0.124	0.1272	0.124	2059.5	2.2	3069
Phala_m@20r	2.10E+05	20.3	0.1275	0.137	0.1275	0.137	2063.2	2.4	2511
Phala_m@21r	5.92E+05	24.1	0.1272	0.111	0.1272	0.111	2059.6	2.0	3819
Phala_m@22r	3.60E+05	21.0	0.1273	0.115	0.1273	0.115	2060.6	2.0	3584
Phala_m@23r	8.14E+05	27.3	0.1271	0.102	0.1271	0.102	2057.9	1.8	4497
Phala_m@24r	5.72E+05	24.1	0.1274	0.104	0.1274	0.104	2062.9	1.8	4390

[a] The values of $^{206}Pb/^{204}Pb_m$ and $^{207}Pb/^{206}Pb_m$ are the measured values.
[b] The value of $^{207}Pb/^{206}Pb_c$ is the calculated value after ^{204}Pb correction.

$^{207}Pb/^{206}Pb = 0.87 \pm 0.05$, which overlap with the range of Phanerozoic terrestrial Pb [*Stacey and Kramers*, 1975]. For SIMS measurements in this study, uncertainties of $(^{207}Pb/^{206}Pb)_m$ vary from 0.1 to 0.8%, and $(^{204}Pb/^{206}Pb)_m$ from 10 to 40%.

[27] Figure 5 illustrates the relationship between uncertainties of the radiogenic $^{207}Pb/^{206}Pb$ ages of 2060 Ma, 560 Ma and 160 Ma and the measured $^{206}Pb/^{204}Pb$ values, along with assigned uncertainties of measured $^{207}Pb/^{206}Pb$ and $^{206}Pb/^{204}Pb$. It is clearly shown that uncertainty of $^{207}Pb/^{206}Pb$ age by SIMS measurements are derived predominantly from the uncertainty of $^{207}Pb/^{206}Pb$ and the measured $^{206}Pb/^{204}Pb$ values. For SIMS measurements with $^{207}Pb/^{206}Pb$ error $\geq$0.2% and $^{206}Pb/^{204}Pb$ error $\geq$10%, uncertainties of common Pb compositions have little or negligible contribution to the final $^{207}Pb/^{206}Pb$ age uncertainty when the measured $^{206}Pb/^{204}Pb$ values exceed 10,000. In contrast, when $^{206}Pb/^{204}Pb$ error $\leq$2% (typical of TIMS measurements), uncertainties of common Pb compositions can affect the $^{207}Pb/^{206}Pb$ age uncertainty significantly when the measured $^{206}Pb/^{204}Pb$ value <10,000.

4.5. Correction of Instrumental Mass Fractionation of Pb Isotopes

[28] During the multicollector mode measurements, a constant $^{90}Zr_2^{16}O^+$ signal ($\sim$1.0 $\times$ 10^5 cps) was used to calibrate the secondary ion yields of each of the EMs on the movable trolleys relative to the axial EM. The yields of all EMs were further fine-tuned against the repeated $^{207}Pb/^{206}Pb$ measurements of Phalaborwa baddeleyite.

[29] Previous SIMS measurements of Pb isotope compositions of zircons and baddeleyite have demonstrated that instrumental mass fractionation of Pb isotopes is negligible [e.g., *Compston et al.*, 1984; *Whitehouse et al.*, 1997; *Wingate and Giddings*, 2000; *Li et al.*, 2005]. In fact, it is very difficult to make an accurate measurement of instrumental mass fractionation within relatively poor precisions of Pb isotope ratios by using monocollector mode SIMS, because of low Pb concentrations in zircon and baddeleyite and the difficulty of resolving any PbH isobars (M/ΔM = 33,000). A number of studies have shown that measurements of $^{207}Pb/^{206}Pb$ ratio from well-characterized reference zircons and baddeleyites are generally in agreement with the recommended values within analytical errors, and there appears to be a mutual cancellation of the hydrides and fractionation that raise and lower the $^{207}Pb/^{206}Pb$

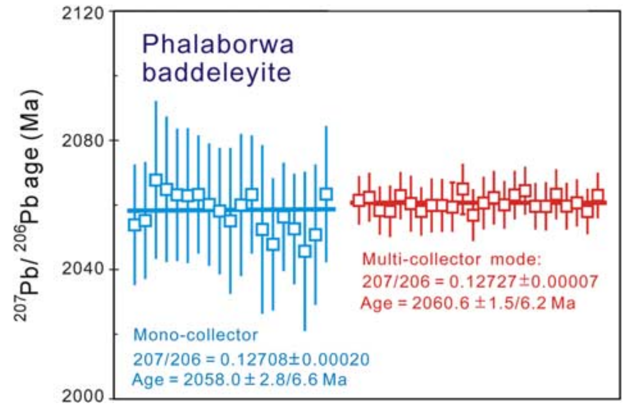

Figure 6. Comparison of weighted average $^{207}Pb/^{206}Pb$ ages for Phalaborwa baddeleyite determined by Cameca IMS-1280 SIMS using monocollector and multicollector modes. Uncertainties are 95% confidence level. Data point error bars are 2σ.

respectively [e.g., *Whitehouse et al.*, 1997; *Ireland and Williams*, 2003]. In practice, instrumental mass fractionation corrections were generally not made in SIMS zircon and baddeleyite Pb/Pb age determination. Our measurements of the well-characterized Phalaborwa baddeleyite by using monocollector mode yield a weighted mean $^{207}Pb/^{206}Pb$ ratio of 0.12708 ± 0.00020 (95% confidence interval, hereafter), corresponding to an age of 2058.0 ± 2.8/6.6 Ma (Table 1 and Figure 5). This age is in agreement within errors with the age of 2059.60 ± 0.35 Ma (excluding decay constant errors) determined by TIMS [*Heaman and LeCheminant*, 1993; *Heaman*, 2009]. Measurements of the Phalaborwa baddeleyite by using multicollector mode give more precise $^{207}Pb/^{206}Pb$ ratio of 0.12727 ± 0.00007 corresponding to an age of 2060.6 ± 1.0/6.1 Ma (Figure 6), indicating negligible instrumental mass fractionation associated with the sputtering process. No correction of instrumental mass fractionation was made on $^{207}Pb/^{206}Pb$ measurement of zircons. A factor of 1.000456, the ratio of our measured $^{207}Pb/^{206}Pb$ (0.12727)/the recommended $^{207}Pb/^{206}Pb$ (0.127212), was applied to fine-tune the yield of EM at H1 (detecting ^{207}Pb) relative to the axial EM (detecting ^{206}Pb).

4.6. ID-TIMS Methods for Qinghu Zircon

[30] Six single zircons that were free of inclusions and internal fractures were selected for analysis. Five grains were annealed at 850°C for 48 h and dissolved in two steps following the chemical abrasion method of *Mattinson* [2005]. The first dissolution step used HF and HNO_3 in a 180°C oven for 12 h. The liquid was discarded, and the

Table 2. Zircon U-Pb Data Determined by Monocollector SIMS Mode

Sample Spot	U (ppm)	Th (ppm)	Th/U	$^{206}Pb/^{204}Pb_m$ [a]	f_{206} [b] (%)	$^{207}Pb/^{206}Pb$	±1σ (%)	$^{207}Pb/^{235}U$	±1σ (%)	$^{206}Pb/^{238}U$	±1σ (%)	$t_{207/206}$ (Ma)	±1σ	$t_{207/235}$ (Ma)	±1σ	$t_{206/238}$ (Ma)	±1σ
BR266																	
BR266@1	974	192	0.20	8.29E+4	0.02	0.0589	0.36	0.732	1.33	0.0901	1.28	563.3	7.8	557.5	5.7	556.0	6.8
BR266@2	978	195	0.21	8.90E+4	0.02	0.0591	0.36	0.722	1.33	0.0887	1.27	569.7	7.9	552.1	5.7	547.8	6.7
BR266@3	979	195	0.21	6.37E+4	0.03	0.0589	0.37	0.725	1.33	0.0893	1.27	562.8	8.1	553.4	5.7	551.2	6.7
BR266@4	990	198	0.21	1.01E+5	0.02	0.0589	0.58	0.724	1.41	0.0892	1.29	563.7	12.6	553.2	6.0	550.6	6.8
BR266@5	1040	224	0.22	5.06E+4	0.04	0.0592	0.46	0.735	1.36	0.0900	1.28	574.6	10.0	559.4	5.9	555.7	6.8
BR266@6	1049	228	0.23	3.90E+4	0.05	0.0593	0.62	0.735	1.42	0.0899	1.27	577.4	13.5	559.5	6.1	555.2	6.8
BR266@7	1040	222	0.22	6.40E+4	0.03	0.0592	0.64	0.736	1.43	0.0901	1.27	574.3	14.0	559.8	6.2	556.3	6.8
BR266@8	1045	223	0.22	6.04E+4	0.03	0.0588	0.43	0.732	1.34	0.0903	1.27	560.8	9.4	557.8	5.8	557.1	6.8
BR266@9	1041	224	0.22	3.25E+4	0.06	0.0593	0.44	0.732	1.35	0.0895	1.27	578.2	9.6	557.5	5.8	552.4	6.7
BR266@10	1060	235	0.23	8.07E+4	0.02	0.0592	0.51	0.743	1.42	0.0910	1.32	575.9	11.0	564.3	6.2	561.5	7.1
BR266@11	988	199	0.21	7.59E+4	0.02	0.0589	0.37	0.731	1.33	0.0901	1.27	562.2	8.1	557.2	5.7	556.0	6.8
BR266@12	1079	240	0.23	4.92E+4	0.04	0.0592	0.46	0.737	1.35	0.0903	1.27	575.2	9.9	560.7	5.9	557.1	6.8
BR266@13	1077	239	0.23	7.02E+4	0.03	0.0591	0.46	0.737	1.36	0.0904	1.28	571.5	9.9	560.5	5.9	557.8	6.8
BR266@14	1066	237	0.23	3.70E+4	0.05	0.0591	0.46	0.737	1.36	0.0903	1.28	572.1	10.0	560.4	5.9	557.6	6.8
BR266@15	1064	234	0.23	4.74E+4	0.04	0.0591	0.48	0.737	1.36	0.0904	1.27	572.1	10.3	560.5	5.9	557.6	6.8
BR266@16	1059	233	0.23	3.74E+4	0.05	0.0588	0.56	0.738	1.39	0.0911	1.27	558.2	12.2	561.3	6.0	562.1	6.9
BR266@17	1070	239	0.23	3.88E+4	0.05	0.0593	0.46	0.735	1.36	0.0900	1.28	577.3	10.0	559.7	5.9	555.4	6.8
BR266@18	1069	238	0.23	3.25E+4	0.06	0.0589	0.58	0.734	1.41	0.0905	1.28	561.8	12.6	559.1	6.1	558.4	6.9
BR266@19	1053	231	0.23	5.41E+4	0.03	0.0589	0.52	0.733	1.39	0.0902	1.29	564.5	11.2	558.4	6.0	556.9	6.9
BR266@20	994	224	0.23	5.78E+4	0.03	0.0591	0.54	0.741	1.38	0.0909	1.27	572.1	11.7	563.2	6.0	561.0	6.8
BR266@21	1007	229	0.24	4.07E+4	0.05	0.0589	0.48	0.741	1.36	0.0913	1.28	562.2	10.4	563.1	5.9	563.3	6.9
BR266@22	1002	225	0.23	2.35E+4	0.08	0.0584	0.67	0.723	1.45	0.0898	1.28	544.3	14.6	552.3	6.2	554.3	6.8
BR266@23	995	221	0.23	5.56E+4	0.03	0.0588	0.59	0.729	1.42	0.0900	1.29	559.7	12.7	556.2	6.1	555.3	6.9
BR266@24	986	224	0.24	3.29E+4	0.06	0.0584	0.48	0.732	1.36	0.0909	1.27	545.6	10.4	557.8	5.8	560.7	6.8
BR266@25	1004	204	0.21	6.80E+4	0.03	0.0587	0.38	0.727	1.33	0.0899	1.27	554.9	8.4	554.9	5.7	554.9	6.8
BR266@26	1002	205	0.21	6.26E+4	0.03	0.0589	0.38	0.725	1.33	0.0893	1.27	561.8	8.2	553.5	5.7	551.4	6.7
BR266@27	1003	202	0.21	8.69E+4	0.02	0.0587	0.37	0.721	1.33	0.0891	1.27	554.6	8.0	551.3	5.7	550.5	6.7
BR266@28	982	198	0.21	1.15E+4	0.02	0.0589	0.37	0.722	1.34	0.0889	1.29	563.9	8.0	551.8	5.7	548.9	6.8
BR266@29	980	194	0.21	7.50E+4	0.02	0.0591	0.40	0.723	1.34	0.0887	1.27	571.7	8.7	552.5	5.7	547.8	6.7
BR266@30	975	193	0.21	8.05E+4	0.02	0.0592	0.49	0.727	1.38	0.0892	1.30	573.2	10.6	555.1	5.9	550.6	6.8
Plešovice																	
Ples@1	516	46	0.09	1.38E+4	0.14	0.0532	1.48	0.396	1.92	0.0540	1.22	337.9	33.2	339.0	5.4	339.2	3.9
Ples@2	2321	274	0.12	9.62E+4	0.02	0.0529	0.54	0.401	1.32	0.0550	1.20	324.5	12.2	342.3	3.9	345.0	4.1
Ples@3	871	91	0.10	2.62E+4	0.07	0.0528	0.97	0.393	1.55	0.0539	1.20	322.3	22.0	336.5	4.4	338.6	3.9
Ples@4	795	78	0.10	3.10E+4	0.06	0.0533	1.03	0.398	1.58	0.0541	1.21	341.4	23.1	339.9	4.5	339.7	3.9
Ples@5	528	49	0.09	1.39E+4	0.13	0.0527	1.36	0.387	1.81	0.0533	1.20	317.3	30.5	332.4	5.2	334.5	3.9
Ples@6	965	107	0.11	3.68E+4	0.05	0.0527	1.13	0.393	1.65	0.0542	1.21	314.4	25.5	336.9	4.8	340.2	4.0
Ples@7	459	40	0.09	1.92E+4	0.10	0.0533	1.04	0.396	1.64	0.0539	1.26	342.1	23.4	338.9	4.7	338.4	4.2
Ples@8	799	73	0.09	2.18E+4	0.09	0.0538	0.79	0.395	1.48	0.0533	1.26	362.2	17.7	338.2	4.3	334.8	4.1
Ples@9	505	42	0.08	2.17E+4	0.09	0.0538	1.11	0.393	1.68	0.0531	1.26	361.6	24.9	336.9	4.8	333.4	4.1

Table 2. (continued)

Sample Spot	U (ppm)	Th (ppm)	Th/U	$^{206}Pb/^{204}Pb_m$ [a]	f_{206} [b] (%)	$^{207}Pb/^{206}Pb$	±1σ (%)	$^{207}Pb/^{235}U$	±1σ (%)	$^{206}Pb/^{238}U$	±1σ (%)	$t_{207/206}$ (Ma)	±1σ	$t_{207/235}$ (Ma)	±1σ	$t_{206/238}$ (Ma)	±1σ
Ples@10	522	45	0.09	1.45E+4	0.13	0.0536	1.09	0.393	1.67	0.0532	1.26	352.8	24.5	336.3	4.8	333.9	4.1
PleS@11	798	67	0.08	1.55E+4	0.12	0.0526	0.92	0.385	1.56	0.0531	1.26	311.9	20.8	330.9	4.4	333.6	4.1
Ples@12	474	38	0.08	2.17E+4	0.09	0.0545	1.01	0.400	1.61	0.0532	1.26	390.3	22.5	341.5	4.7	334.4	4.1
Ples@13	449	35	0.08	1.96E+4	0.10	0.0524	1.34	0.390	1.84	0.0539	1.26	305.0	30.3	334.4	5.3	338.6	4.2
Ples@14	530	44	0.08	3.61E+4	0.05	0.0530	0.86	0.395	1.53	0.0540	1.26	330.3	19.4	337.7	4.4	338.8	4.2
Ples@15	530	44	0.08	2.66E+4	0.07	0.0538	0.87	0.396	1.53	0.0535	1.26	360.6	19.6	338.9	4.4	335.8	4.1
Ples@16	469	38	0.08	1.51E+4	0.12	0.0529	1.00	0.387	1.61	0.0531	1.26	326.2	22.5	332.3	4.6	333.2	4.1
Ples@17	600	54	0.09	2.31E+4	0.08	0.0525	0.85	0.386	1.52	0.0533	1.26	305.2	19.3	331.3	4.3	335.0	4.1
Ples@18	850	82	0.10	3.80E+4	0.05	0.0538	0.79	0.400	1.49	0.0539	1.26	361.7	17.8	341.4	4.3	338.4	4.1
Ples@19	808	77	0.10	4.86E+4	0.04	0.0533	0.80	0.393	1.51	0.0535	1.28	341.5	18.1	336.7	4.3	336.0	4.2
Ples@20	810	88	0.11	3.47E+4	0.05	0.0543	0.77	0.399	1.47	0.0534	1.26	383.4	17.2	341.3	4.3	335.1	4.1
Ples@21	898	84	0.09	8.69E+3	0.22	0.0524	1.19	0.383	1.76	0.0530	1.30	303.2	27.0	329.2	5.0	332.9	4.2
Ples@22	607	59	0.10	1.68E+4	0.11	0.0541	1.23	0.394	1.83	0.0529	1.36	374.9	27.3	337.6	5.3	332.3	4.4
Ples@23	817	90	0.11	6.04E+4	0.03	0.0541	0.75	0.399	1.47	0.0535	1.27	375.0	16.7	340.9	4.3	335.9	4.2
Ples@24	537	46	0.09	4.84E+3	0.39	0.0529	1.01	0.391	1.65	0.0536	1.31	324.5	22.8	334.9	4.7	336.4	4.3
Ples@25	1357	119	0.09	4.48E+4	0.04	0.0534	0.60	0.400	1.39	0.0544	1.26	344.9	13.5	341.8	4.0	341.4	4.2
Ples@26	1106	92	0.08	3.07E+4	0.06	0.0533	0.55	0.402	1.37	0.0547	1.26	340.2	12.3	343.0	4.0	343.4	4.2
Ples@27	1009	104	0.10	1.60E+4	0.12	0.0525	0.74	0.395	1.46	0.0546	1.26	308.1	16.9	338.1	4.2	342.5	4.2
Ples@28	741	67	0.09	7.19E+4	0.03	0.0532	0.64	0.400	1.42	0.0546	1.26	337.2	14.5	341.9	4.1	342.5	4.2
Ples@29	445	30	0.07	9.50E+4	0.02	0.0535	0.98	0.396	1.59	0.0536	1.26	350.8	22.0	338.6	4.6	336.8	4.1
Ples@30	536	45	0.08	6.52E+4	0.03	0.0530	0.70	0.393	1.44	0.0538	1.26	328.7	15.7	336.6	4.1	337.8	4.1
Qinghu																	
QH@1	1764	959	0.543	6.13E+4	0.03	0.0500	0.69	0.176	1.38	0.0256	1.20	196.5	15.8	165.0	2.1	162.8	1.9
QH@2	1023	515	0.504	1.60E+4	0.12	0.0494	1.07	0.170	1.61	0.0250	1.20	166.7	24.9	159.4	2.4	159.0	1.9
QH@3	1111	552	0.497	2.29E+4	0.08	0.0490	0.91	0.172	1.52	0.0255	1.21	146.8	21.3	161.3	2.2	162.3	1.9
QH@4	725	345	0.476	1.91E+4	0.10	0.0489	1.18	0.169	1.69	0.0250	1.21	144.5	27.4	158.1	2.4	159.0	1.9
QH@5	1352	737	0.545	2.66E+4	0.07	0.0492	0.89	0.173	1.50	0.0255	1.20	157.0	20.8	162.0	2.2	162.3	1.9
QH@6	1835	712	0.388	1.06E+5	0.02	0.0499	0.58	0.179	1.34	0.0260	1.21	188.9	13.3	167.1	2.1	165.6	2.0
QH@7	709	282	0.398	3.75E+4	0.05	0.0492	0.99	0.171	1.57	0.0252	1.22	156.2	23.1	160.2	2.3	160.5	1.9
QH@8	684	293	0.429	2.31E+4	0.08	0.0495	1.32	0.171	1.80	0.0251	1.23	169.4	30.6	160.3	2.7	159.7	1.9
QH@9	1213	551	0.454	1.94E+4	0.10	0.0492	0.86	0.170	1.48	0.0250	1.20	157.4	19.9	159.2	2.2	159.3	1.9
QH@10	982	593	0.604	2.20E+4	0.09	0.0483	1.11	0.168	1.64	0.0252	1.21	115.4	26.0	157.7	2.4	160.5	1.9
QH@11	1317	647	0.491	4.96E+4	0.04	0.0494	0.89	0.171	1.50	0.0251	1.21	165.2	20.7	160.1	2.2	159.8	1.9
QH@12	811	509	0.627	3.76E+4	0.05	0.0492	0.94	0.170	1.56	0.0250	1.25	159.1	21.8	159.3	2.3	159.3	2.0
QH@13	966	435	0.450	5.86E+4	0.03	0.0498	0.86	0.173	1.48	0.0253	1.21	183.5	19.8	162.2	2.2	160.8	1.9
QH@14	717	327	0.456	3.73E+4	0.05	0.0498	1.16	0.172	1.68	0.0251	1.21	185.1	26.9	161.3	2.5	159.7	1.9
QH@15	994	424	0.427	4.08E+4	0.05	0.0497	0.84	0.171	1.47	0.0249	1.21	181.0	19.5	160.2	2.2	158.8	1.9
QH@16	967	365	0.377	5.5 E+4	0.03	0.0490	0.85	0.168	1.48	0.0249	1.21	148.0	19.8	157.7	2.2	158.3	1.9
QH@17	2413	1768	0.733	7.30E+4	0.03	0.0490	0.63	0.168	1.36	0.0249	1.20	147.7	14.7	158.1	2.0	158.8	1.9
QH@18	878	373	0.425	5.51E+4	0.03	0.0490	1.05	0.167	1.60	0.0248	1.21	147.6	24.4	157.0	2.3	157.6	1.9
QH@19	956	409	0.428	3.62E+4	0.05	0.0488	0.85	0.169	1.48	0.0251	1.21	139.1	19.8	158.5	2.2	159.8	1.9

Table 2. (continued)

Sample Spot	U (ppm)	Th (ppm)	Th/U	$^{206}Pb/^{204}Pb_m$ [a]	f_{206} [b] (%)	$^{207}Pb/^{206}Pb$	±1σ (%)	$^{207}Pb/^{235}U$	±1σ (%)	$^{206}Pb/^{238}U$	±1σ (%)	$t_{207/206}$ (Ma)	±1σ	$t_{207/235}$ (Ma)	±1σ	$t_{206/238}$ (Ma)	±1σ
QH@20	547	250	0.458	3.54E+4	0.05	0.0489	1.13	0.166	1.66	0.0246	1.21	144.4	26.4	156.0	2.4	156.7	1.9
QH@21	791	335	0.423	5.30E+4	0.04	0.0489	0.91	0.169	1.51	0.0251	1.21	143.3	21.3	158.9	2.2	160.0	1.9
QH@22	628	338	0.538	2.31E+4	0.08	0.0494	1.16	0.167	1.67	0.0246	1.20	165.4	26.9	156.9	2.4	156.4	1.9
QH@23	969	460	0.475	5.26E+4	0.04	0.0495	0.83	0.170	1.47	0.0248	1.21	173.3	19.3	159.2	2.2	158.2	1.9
QH@24	803	399	0.497	6.57E+4	0.03	0.0496	0.92	0.170	1.53	0.0248	1.20	174.9	21.3	159.1	2.2	158.0	1.9
QH@25	840	366	0.436	3.96E+4	0.05	0.0489	0.90	0.169	1.50	0.0251	1.20	140.7	20.9	158.4	2.2	159.5	1.9
QH@26	1156	506	0.437	6.60E+4	0.03	0.0485	0.76	0.166	1.42	0.0249	1.20	121.9	17.7	156.0	2.1	158.3	1.9
QH@27	791	379	0.479	3.08E+4	0.06	0.0490	0.97	0.168	1.55	0.0248	1.20	147.5	22.6	157.3	2.3	158.0	1.9
QH@28	526	237	0.452	3.65E+4	0.05	0.0492	1.18	0.170	1.69	0.0251	1.21	155.6	27.4	159.5	2.5	159.8	1.9
QH@29	727	310	0.427	3.03E+4	0.06	0.0485	1.03	0.168	1.58	0.0251	1.20	122.3	24.0	157.4	2.3	159.8	1.9
QH@30	1009	525	0.520	4.02E+4	0.05	0.0488	1.70	0.168	2.09	0.0249	1.21	140.6	39.5	157.5	3.1	158.7	1.9

[a] The value of $^{206}Pb/^{204}Pb_m$ is the measured value.
[b] f_{206} is the percentage of common ^{206}Pb in total ^{206}Pb.

remaining grains were rinsed and cleaned in HCl and HNO_3. A mixed ^{205}Pb-^{233}U-^{235}U tracer solution (ET535) was added to the microbombs for isotope dilution determination of Pb and U abundances. Final dissolution used HF and HNO_3 at 240°C and included a sixth, untreated grain that was analyzed to monitor absolute Pb and U concentrations. Additional details are given in the notes to Table 4.

5. Analytical Results

[31] Three zircon samples from different rock types with ages ranging from the latest Neoproterozoic to middle Jurassic were chosen for analysis in this study. Zircon grains, together with a zircon U-Pb standard 91500 and Phalaborwa baddeleyite, were cast in transparent epoxy mount, which was then polished to section the crystals in half for analysis. Zircons were documented with transmitted and reflected light micrographs as well as cathodoluminescence (CL) images to reveal their internal structures, and the mount was vacuum-coated with high-purity gold prior to SIMS analysis. SIMS U-Pb and Pb/Pb data by using monocollector and Pb/Pb data by using multicollector modes are presented in Tables 2 and 3, respectively.

5.1. BR266 Zircon

[32] This is a gem-quality zircon from Sri Lanka and used as an ion microprobe reference material for U-Pb zircon dating by the Geological Survey of Canada. It has a slightly discordant $^{206}Pb/^{238}U$ and $^{207}Pb/^{206}Pb$ ages dated by TIMS at 559.0 ± 0.3 Ma and 562.2 ± 0.5 Ma (excluding decay constant errors), respectively [*Stern*, 2001; *Stern and Amelin*, 2003]. These dates overlap within error of chemically abraded TIMS dates (559.27 ± 0.11 Ma and 562.00 ± 0.50 Ma, respectively) produced by *Schoene et al.* [2006].

[33] Thirty measurements of U-Pb isotopes were conducted on BR266 zircon by using monocollector mode, and the data are plotted in Figure 7a. The measured U-Pb isotopes are marginally concordant when the decay constant error is included. The weighted mean of $^{207}Pb/^{206}Pb$, $^{207}Pb/^{235}U$ and $^{206}Pb/^{238}U$ ratios is 0.058966 ± 0.000096, 0.7313 ± 0.0036 and 0.08997 ± 0.00041, respectively, corresponding to age of 565.7 ± 3.5/5.8 Ma, 557.4 ± 2.1/2.2 Ma and 555.3 ± 2.4/2.5 Ma, respectively. A U-Pb concordia age is calculated at 558.6 ± 2.1 (excluding decay constant errors), or 557.2 ± 2.3 Ma (including decay constant errors),

Table 3. Zircon Pb/Pb Data Determined by Multicollector SIMS Mode

Sample Spot	$^{206}Pb/^{204}Pb_m$ [a]	±1σ (%)	$^{207}Pb/^{206}Pb_m$ [a]	±1σ (%)	$^{207}Pb/^{206}Pb_c$ [b]	±1σ (%)	$t_{207/206}$ (Ma)	±1σ	^{207}Pb (cps)
BR266									
BR266@1r	2.96E+05	23.0	0.05892	0.195	0.05887	0.196	562.1	4.3	1158
BR266@2r	3.95E+05	26.5	0.05905	0.202	0.05901	0.203	567.4	4.4	1129
BR266@3r	3.53E+05	22.8	0.05879	0.196	0.05875	0.197	558.0	4.3	1145
BR266@4r	9.57E+05	42.2	0.05893	0.195	0.05891	0.196	563.8	4.3	1160
BR266@5r	2.10E+05	19.5	0.05910	0.196	0.05903	0.198	568.2	4.3	1150
BR266@6r	3.60E+05	23.7	0.05883	0.197	0.05879	0.197	559.3	4.3	1142
BR266@7r	1.85E+05	18.5	0.05890	0.196	0.05882	0.198	560.3	4.3	1147
BR266@8r	3.92E+05	24.2	0.05900	0.196	0.05896	0.197	565.7	4.3	1147
BR266@9r	5.77E+05	31.7	0.05903	0.195	0.05900	0.196	567.2	4.3	1161
BR266@10r	4.27E+05	27.5	0.05919	0.198	0.05916	0.199	572.9	4.3	1126
BR266@11r	3.37E+05	23.4	0.05892	0.196	0.05888	0.197	562.5	4.3	1151
BR266@12r	3.35E+05	23.4	0.05904	0.197	0.05899	0.197	566.8	4.3	1144
BR266@13r	2.20E+05	20.3	0.05886	0.196	0.05879	0.198	559.4	4.3	1148
BR266@14r	2.99E+05	22.8	0.05896	0.209	0.05891	0.210	563.8	4.6	1098
BR266@15r	3.88E+05	25.8	0.05899	0.228	0.05895	0.228	565.3	5.0	1046
BR266@16r	4.67E+05	29.4	0.05903	0.205	0.05899	0.206	566.9	4.5	1051
BR266@17r	3.52E+05	24.1	0.05869	0.205	0.05865	0.205	554.0	4.5	1055
BR266@18r	3.00E+05	22.2	0.05907	0.205	0.05903	0.206	568.0	4.5	1053
BR266@19r	1.97E+05	20.7	0.05890	0.205	0.05883	0.207	560.6	4.5	1053
BR266@20r	5.66E+05	34.3	0.05898	0.205	0.05895	0.206	565.3	4.5	1051
BR266@21r	2.37E+05	21.2	0.05897	0.203	0.05891	0.205	563.9	4.5	1071
BR266@22r	2.00E+05	21.1	0.05892	0.216	0.05885	0.217	561.4	4.7	1052
BR266@23r	2.66E+05	22.9	0.05884	0.203	0.05878	0.205	559.0	4.5	1067
BR266@24r	3.16E+05	26.1	0.05885	0.205	0.05881	0.206	559.9	4.5	1052
BR266@25r	1.79E+05	18.4	0.05887	0.204	0.05879	0.206	559.3	4.5	1063
Plešovice									
Ples@1r	7.58E+04	20.3	0.05354	0.335	0.05334	0.344	343.4	7.8	391
Ples@2r	1.57E+04	11.6	0.05416	0.388	0.05322	0.445	338.2	10.0	325
Ples@3r	1.42E+05	15.7	0.05339	0.200	0.05329	0.203	341.2	4.6	1100
Ples@4r	1.06E+05	19.5	0.05361	0.284	0.05347	0.289	349.0	6.5	545
Ples@5r	1.76E+05	23.7	0.05324	0.280	0.05316	0.283	335.5	6.4	558
Ples@6r	1.48E+05	20.7	0.05343	0.248	0.05333	0.251	342.9	5.7	715
Ples@7r	1.38E+05	23.5	0.05326	0.313	0.05315	0.318	335.2	7.2	447
Ples@8r	1.04E+05	21.2	0.05347	0.352	0.05333	0.357	342.9	8.1	355
Ples@9r	6.15E+04	18.4	0.05339	0.358	0.05315	0.369	335.2	8.4	343
Ples@10r	1.54E+05	25.9	0.05347	0.304	0.05337	0.308	344.7	7.0	476
PleS@11r	1.31E+05	22.8	0.05308	0.338	0.05296	0.342	327.3	7.8	386
Ples@12r	1.66E+05	25.5	0.05355	0.322	0.05346	0.325	348.5	7.3	424
Ples@13r	3.56E+04	11.5	0.05372	0.317	0.05331	0.332	341.9	7.5	555
Ples@14r	6.93E+04	12.6	0.05322	0.249	0.05301	0.256	329.2	5.8	777
Ples@15r	4.35E+04	10.8	0.05338	0.249	0.05304	0.260	330.5	5.9	709
Ples@16r	3.15E+04	13.4	0.05336	0.348	0.05290	0.370	324.3	8.4	363
Ples@17r	1.00E+05	22.4	0.05342	0.314	0.05327	0.321	340.4	7.3	445
Ples@18r	4.19E+04	11.1	0.05388	0.263	0.05353	0.275	351.5	6.2	633
Ples@19r	1.73E+05	24.1	0.05329	0.306	0.05320	0.309	337.4	7.0	467
Ples@20r	1.67E+05	20.2	0.05330	0.233	0.05321	0.236	337.7	5.3	806
Ples@21r	1.23E+05	23.4	0.05339	0.288	0.05327	0.294	340.4	6.7	528
Ples@22r	1.02E+05	23.5	0.05343	0.344	0.05329	0.351	341.0	7.9	371
Ples@23r	3.18E+05	17.6	0.05337	0.149	0.05332	0.150	342.5	3.4	1980
Ples@24r	2.63E+05	25.3	0.05337	0.252	0.05331	0.253	342.2	5.7	695
Ples@25r	1.04E+05	20.3	0.05320	0.299	0.05306	0.305	331.3	6.9	491
Qinghu_S1									
QH1@1r	4.92E+04	20.4	0.04941	0.449	0.04911	0.469	153	11	216
QH1@2r	6.32E+04	21.7	0.04935	0.468	0.04912	0.481	154	11	207
QH1@3r	5.47E+04	24.1	0.04942	0.536	0.04915	0.555	155	13	153
QH1@4r	8.09E+04	21.1	0.04957	0.358	0.04939	0.368	166	9	342
QH1@5r	8.24E+04	25.3	0.04937	0.446	0.04919	0.457	157	11	219
QH1@6r	9.43E+04	24.1	0.04973	0.429	0.04958	0.437	175	10	239

Table 3. (continued)

Sample Spot	$^{206}Pb/^{204}Pb_m$ [a]	±1σ (%)	$^{207}Pb/^{206}Pb_m$ [a]	±1σ (%)	$^{207}Pb/^{206}Pb_c$ [b]	±1σ (%)	$t_{207/206}$ (Ma)	±1σ	^{207}Pb (cps)
QH1@7r	7.56E+04	23.4	0.04917	0.442	0.04897	0.453	146	11	224
QH1@8r	2.25E+04	15.0	0.05015	0.451	0.04950	0.499	172	12	216
QH1@9r	9.60E+04	29.1	0.04975	0.476	0.04960	0.486	176	11	193
QH1@10r	3.23E+04	24.8	0.04936	0.642	0.04890	0.688	143	16	106
QH1@11r	8.64E+04	18.4	0.04930	0.301	0.04913	0.309	154	7	484
QH1@12r	3.72E+04	23.4	0.04964	0.581	0.04925	0.616	160	14	131
QH1@13r	4.08E+04	19.1	0.04943	0.488	0.04907	0.511	151	12	184
QH1@14r	7.06E+04	22.3	0.04976	0.398	0.04956	0.411	174	10	277
QH1@15r	1.45E+05	37.8	0.04948	0.550	0.04938	0.557	166	13	188
QH1@16r	3.55E+04	19.0	0.04957	0.474	0.04915	0.505	155	12	195
QH1@17r	5.82E+04	23.9	0.04957	0.587	0.04932	0.603	163	14	151
QH1@18r	8.35E+04	26.5	0.04918	0.470	0.04900	0.481	148	11	198
QH1@19r	8.79E+04	25.6	0.04931	0.456	0.04914	0.466	155	11	210
QH1@20r	3.94E+04	26.5	0.04973	0.681	0.04935	0.716	165	17	94
QH1@21r	7.96E+04	27.5	0.04922	0.549	0.04903	0.561	149	13	173
QH1@22r	5.36E+04	21.2	0.04973	0.508	0.04946	0.524	170	12	170
QH1@23r	1.22E+05	31.8	0.04955	0.468	0.04943	0.475	168	11	200
QH1@24r	6.15E+04	23.9	0.04986	0.524	0.04962	0.539	177	13	160
QH1@25r	8.43E+04	22.5	0.04909	0.431	0.04892	0.440	144	10	235
QH1@26r	9.80E+04	25.6	0.04946	0.440	0.04931	0.448	163	10	226
QH1@27r	2.59E+04	19.9	0.04959	0.685	0.04902	0.731	149	17	103
QH1@28r	3.93E+04	20.7	0.04964	0.497	0.04927	0.525	161	12	177
Qinghu_S2									
QH2@1r	6.28E+04	25.6	0.04921	0.549	0.04898	0.566	147	13	145
QH2@2r	9.10E+04	29.3	0.04930	0.497	0.04914	0.508	155	12	177
QH2@3r	9.58E+04	31.5	0.04939	0.507	0.04924	0.518	159	12	170
QH2@4r	4.40E+04	24.2	0.04983	0.634	0.04950	0.659	172	15	109
QH2@5r	4.02E+04	22.8	0.04982	0.595	0.04945	0.623	169	15	124
QH2@6r	2.59E+04	19.9	0.04949	0.618	0.04892	0.667	144	16	120
QH2@7r	5.05E+04	25.6	0.04938	0.610	0.04909	0.632	152	15	117
QH2@8r	2.83E+05	34.6	0.04967	0.328	0.04961	0.331	177	8	407
QH2@9r	5.69E+04	20.3	0.04953	0.493	0.04927	0.507	161	12	180
QH2@10r	4.71E+04	24.9	0.04960	0.509	0.04929	0.536	162	13	169
QH2@11r	9.70E+04	25.5	0.04941	0.439	0.04926	0.447	160	10	227
QH2@12r	4.46E+04	21.4	0.04951	0.474	0.04918	0.498	156	12	194
QH2@13r	3.81E+04	22.5	0.04937	0.551	0.04898	0.583	147	14	144
QH2@14r	5.05E+04	19.9	0.04931	0.449	0.04902	0.467	149	11	217
QH2@15r	4.80E+04	25.6	0.04968	0.593	0.04937	0.617	165	15	125
QH2@16r	1.08E+05	27.7	0.04930	0.430	0.04916	0.438	155	10	348
QH2@17r	4.39E+04	26.5	0.04993	0.642	0.04960	0.671	176	16	106
QH2@18r	4.07E+04	18.8	0.04944	0.480	0.04907	0.504	151	12	203
QH2@19r	4.87E+04	18.7	0.04937	0.451	0.04907	0.468	151	11	215
QH2@20r	7.03E+04	21.2	0.04981	0.452	0.04960	0.462	176	11	215
QH2@21r	3.96E+04	17.6	0.04956	0.456	0.04919	0.478	157	11	211
QH2@22r	4.33E+04	20.7	0.04968	0.554	0.04934	0.576	164	13	151
QH2@23r	3.93E+04	20.3	0.04951	0.527	0.04914	0.553	155	13	161
QH2@24r	3.40E+04	19.7	0.04951	0.533	0.04908	0.566	152	13	154
QH2@25r	6.47E+04	23.5	0.04932	0.519	0.04909	0.533	152	12	219
QH2@26r	4.63E+04	21.3	0.04947	0.486	0.04915	0.508	155	12	186
QH2@27r	3.80E+04	22.4	0.04937	0.532	0.04898	0.565	147	13	155
QH2@28r	2.33E+04	21.2	0.04965	0.747	0.04902	0.805	149	19	79
QH2@29r	6.95E+04	30.0	0.04958	0.498	0.04937	0.516	165	12	176

[a] The values of $^{204}Pb/^{206}Pb_m$ and $^{207}Pb/^{206}Pb_m$ are the measured values.
[b] The value of $^{207}Pb/^{206}Pb_c$ is the calculated value after ^{204}Pb correction.

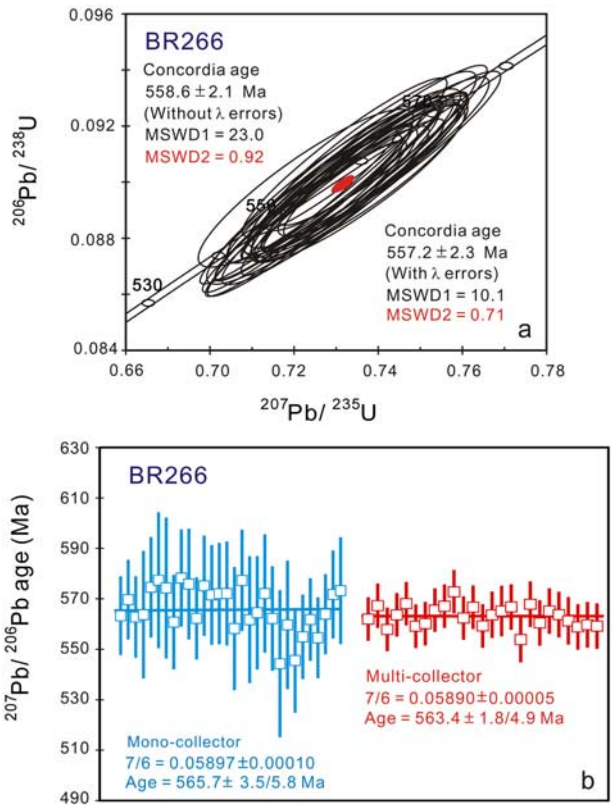

Figure 7. (a) U-Pb concordia diagram showing SIMS analytical data for BR266 zircon. (b) Comparison of weighted average $^{207}Pb/^{206}Pb$ ages for BR266 zircon determined by Cameca IMS-1280 SIMS using monocollector and multicollector modes. Uncertainties are 95% confidence level. MSWD is the mean square of weighted deviates, MSWD1 is the MSWD of concordance, and MSWD2 is the MSWD of concordance plus equivalence. Data point error ellipses/bars are 2σ.

which is lower than the TIMS $^{207}Pb/^{206}Pb$ age of 562.2 ± 0.5 Ma. Our data concur with the slight discordance of U-Pb system of BR266 determined by TIMS [*Stern*, 2001; *Stern and Amelin*, 2003].

[34] Twenty-five measurements of $^{207}Pb/^{206}Pb$ ratios were obtained by multicollector mode, with a weighted mean $^{207}Pb/^{206}Pb$ of 0.05890 ± 0.00005 (0.085%) corresponding to $^{207}Pb/^{206}Pb$ age of 563.4 ± 1.8/4.9 Ma (Figure 7b). This age is in good agreement within errors with the $^{207}Pb/^{206}Pb$ age of 562.2 ± 0.5 Ma determined by TIMS [*Stern*, 2001; *Stern and Amelin*, 2003]. The $^{207}Pb/^{206}Pb$ age uncertainty determined by using multicollector mode is 0.32% (excluding decay constant errors), improved by a factor of ~2 compared to the age uncertainty of 0.62% for thirty measurements obtained by using monocollector mode.

5.2. Plešovice Zircon

[35] This zircon comes from a potassic granulite facies rock at the Plešovice quarry in the southern Bohemian Massif, Czech Republic. It has a concordant U/Pb age with a weighted mean $^{206}Pb/^{238}U$ date of 337.13 ± 0.37 Ma (excluding decay constant error) and a well-defined Hf isotopic composition, and is being considered as a potential zircon reference for U-Pb and Hf isotopic microanalysis [*Sláma et al.*, 2008].

[36] Thirty measurements of U-Pb isotopes were obtained for Plešovice zircon by using monocollector mode. All the analyses are concordant within analytical errors. The weighted mean of $^{207}Pb/^{206}Pb$, $^{207}Pb/^{235}U$ and $^{206}Pb/^{238}U$ ratios is 0.05319 ± 0.00017, 0.3947 ± 0.0022 and 0.05372 ± 0.00024, respectively, corresponding to ages of

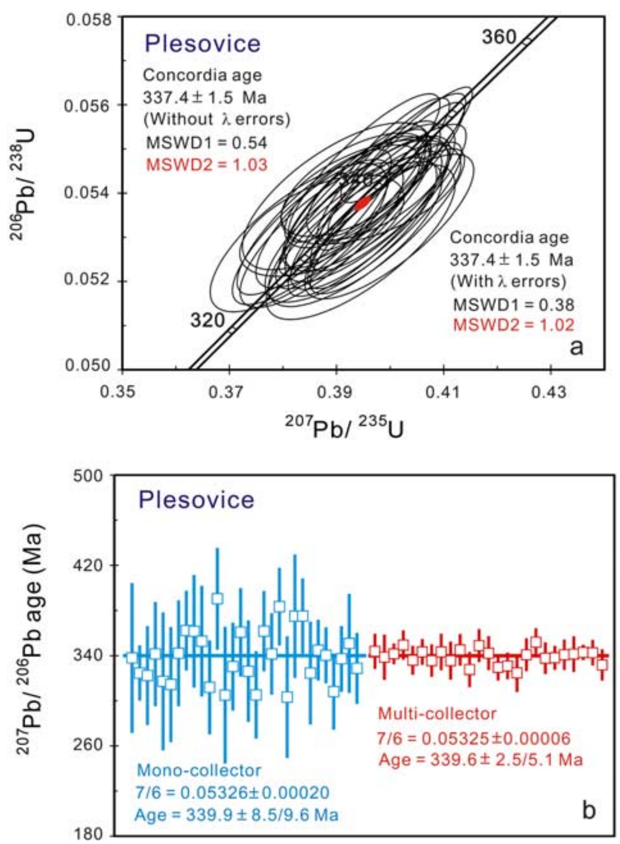

Figure 8. (a) U-Pb concordia diagram showing SIMS analytical data for Plešovice zircon. (b) Comparison of weighted average $^{207}Pb/^{206}Pb$ ages for Plešovice zircon determined by Cameca IMS-1280 SIMS using monocollector and multicollector modes. MSWD is the mean square of weighted deviates, MSWD1 is the MSWD of concordance, and MSWD2 is the MSWD of concordance plus equivalence. Data point error ellipses/bars are 2σ.

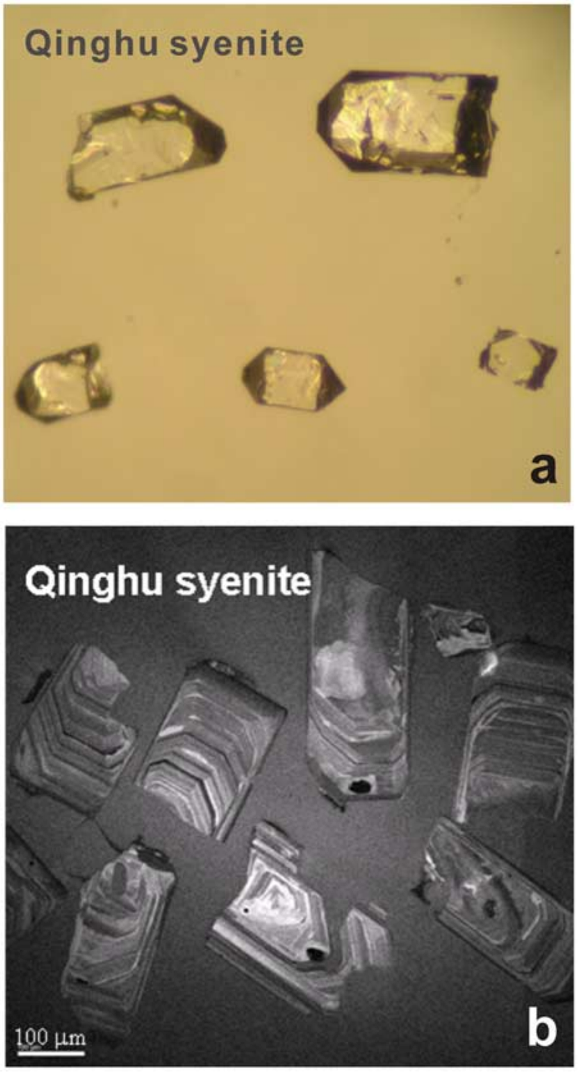

Figure 9. (a) Photomicrographs of five single grains of Qinghu zircon analyzed by CA-TIMS. Grains are arranged left to right, with grains A and B on the top and grains C–E on the bottom. Grain A is 250 microns in length for scale. (b) Cathodoluminescence images for representative Qinghu zircon grains.

340.3 ± 8.4/8.5 Ma, 337.8 ± 1.6/1.7 Ma and 337.3 ± 1.5/1.5 Ma, respectively. A concordia U-Pb age is calculated at 337.4 ± 1.5/1.5 Ma (Figure 8a). Our U-Pb age is in good agreement with the reported ^{206}Pb/^{238}U age of 337.13 ± 0.37 Ma by TIMS [*Sláma et al.*, 2008].

[37] Twenty-five measurements by using multicollector mode yielded indistinguishable ^{207}Pb/^{206}Pb ratios within analytical errors, with a weighted mean of 0.053252 ± 0.000058 (0.11%) corresponding to a ^{207}Pb/^{206}Pb age of 339.6 ±2.5/5.1 Ma (Figure 8b). The ^{207}Pb/^{206}Pb age uncertainty of 0.74% (excluding decay constant error) determined by using multicollector mode is improved by a factor of ∼3 relative to that of 2.5% obtained by using monocollector mode.

5.3. Qinghu Zircon

[38] The Qinghu zircon was separated from a felsic syenite rock at a large quarry in the Qinghu alkaline complex near the border between Guangdong and Guangxi Provinces, South China [*Li et al.*, 2004]. This complex was previously dated at 156 ± 6 Ma by LA-ICPMS [*Li et al.*, 2001]. Zircons from this sample are all euhedral, range mostly from 200 to 500 μm in length, and have length to width ratios of ∼3:1. They are transparent and light brown in color (Figure 9a), showing clear euhedral concentric zoning under CL (Figure 9b).

[39] TIMS data from the five chemically abraded zircons cluster on Concordia (Table 4 and Figure 10) with a weighted mean ^{206}Pb/^{238}U date of 159.38 ± 0.12 Ma (MSWD = 1.6) and a ^{207}Pb/^{235}U date of 159.68 ± 0.22 (MSWD = 0.4). The U-Pb dates agree within the decay constant uncertainties, and the degree of discordance is similar to those from other CA-TIMS dated standards [e.g., *Schoene et al.*, 2006]. The concordia age is 159.45 ± 0.16 Ma (2σ, including decay errors [*Ludwig*, 1998]). Data from the untreated grain display a younger ^{206}Pb/^{238}U date (157.9 Ma) and are interpreted to reflect minor Pb loss.

[40] Thirty analyses by monocollector SIMS mode give concordant U-Pb and Pb-Pb results within analytical errors. The weighted mean of ^{207}Pb/^{206}Pb, ^{207}Pb/^{235}U and ^{206}Pb/^{238}U ratios is 0.04923 ± 0.00016, 0.1700 ± 0.0011 and 0.02506 ± 0.00011, respectively, corresponding to ages of 158.9 ± 7.6/8.7 Ma, 159.45 ± 0.97/0.98 Ma, and 159.56 ± 0.69/0.71 Ma, respectively. The calculated Concordia U-Pb age of 159.5 ± 0.6/0.7 Ma (Figure 11a) is in good agreement with the TIMS data.

[41] ^{207}Pb/^{206}Pb ratios were analyzed by using multicollector SIMS mode in two separated sessions, with sessions 1 and 2 consisting of twenty-eight and twenty-nine measurements, respectively. Both sessions yield indistinguishable weighted mean ^{207}Pb/^{206}Pb ratios within errors: 0.049252 ± 0.000089 (0.18%) and 0.049232 ± 0.000094 (0.19%), corresponding to ^{207}Pb/^{206}Pb ages of 159.8 ± 4.2/6.0 and 158.9 ± 4.5/6.2, respectively (Figure 11b). The ^{207}Pb/^{206}Pb age error determined by multicollector mode is 2.6–2.8% (excluding decay constant error), which is improved by a

Table 4. U-Pb TIMS Zircon Data[a]

Sample	Weight (mcg)	U (ppm)	Sample Pb ppm	Sample Pb pg	Initial Pb ppm	Initial Pb pg	Pb^*/Pb_c	Th/U	Meas. $^{206}Pb/^{204}Pb$	$^{206}Pb/^{204}Pb$	$^{208}Pb/^{206}Pb$	Corrected Atomic Ratios $^{206}Pb/^{238}U$ rad.	$^{206}Pb/^{238}U$ %err	$^{207}Pb/^{235}U$ rad.	$^{207}Pb/^{235}U$ %err	$^{207}Pb/^{206}Pb$ rad.	$^{207}Pb/^{206}Pb$ %err	206/238 Age (Ma)	err	207/235 Age (Ma)	err	207/206 Age (Ma)	Rho
												Qinghu Zircon[b]											
sA CA *st*	13.5	807.0	20.7	280	0.280	3.8	39.5	0.40	2497	4585	0.13	0.025019	(0.21)	0.17020	(0.33)	0.0493	(0.23)	159.30	±0.34	159.59	±0.52	164	0.70
sB CA *st*	24.3	694.6	18.0	436	0.004	0.1	132	0.47	8173	281829	0.15	0.025026	(0.06)	0.17025	(0.17)	0.0493	(0.14)	159.34	±0.10	159.64	±0.27	164	0.51
sC CA *sd*	3.5	1342.3	33.9	118	0.347	1.2	26.6	0.35	1711	6155	0.11	0.025024	(0.09)	0.17054	(0.53)	0.0494	(0.48)	159.33	±0.14	159.89	±0.84	168	0.54
sD CA *sd*	3.5	989.5	25.8	90	0.138	0.5	24.3	0.47	1517	11388	0.15	0.025058	(0.09)	0.17081	(0.68)	0.0494	(0.63)	159.55	±0.14	160.12	±1.09	169	0.64
sE CA *sd*	2.3	1212.8	31.9	72	0.345	0.8	17.9	0.50	1110	5594	0.16	0.025024	(0.10)	0.17085	(0.86)	0.0495	(0.80)	159.33	±0.16	160.15	±1.38	172	0.70
sG *st*	4.7	1105.4	28.6	134	1.103	5.2	15.4	0.37	994	1595	0.12	0.024802	(0.07)	0.16868	(0.48)	0.0493	(0.45)	157.93	±0.12	158.28	±0.77	163	0.54
												Paired Single Daly Run Data											
sA CA *sd*	13.5	807.0	20.7	280	0.256	3.4	39.8	0.40	2512	4635	0.13	0.025045	(0.21)	0.17021	(0.33)	0.0493	(0.24)	159.46	±0.34	159.60	±0.52	162	0.69
sG *sd*	4.7	1105.4	28.6	134	1.052	4.9	15.3	0.37	988	1578	0.12	0.024807	(0.08)	0.16871	(0.51)	0.0493	(0.47)	157.97	±0.13	158.29	±0.80	163	0.54

[a] Samples are as follows: s_, single zircon grain; CA, chemically abraded; *st*, static Pb run; *sd*, single Daly multiplier Pb run. Paired single Daly data are from Daly Pb runs on the same beads after static analysis. Weight is zircon grain weight prior to first step of either CATIMS or total dissolution. U and Pb concentrations for CA method analyses are based on this weight and may be underestimations, depending on how much material was dissolved and leached in the first step. Picograms (pg) sample and initial Pb from the second dissolution step are measured directly. The weights and concentrations from the bulk dissolved grain are all accurate. Sample Pb is sample Pb (radiogenic + initial) corrected for laboratory blank of 3.2 pg; initial Pb is common Pb corrected for laboratory blank of 3.2 pg Pb. Isotopic composition of blank is 18.719 ± 0.97 ($^{206}Pb/^{204}Pb$), 15.662 ± 0.57 ($^{207}Pb/^{204}Pb$), and 38.226 ± 1.42 ($^{208}Pb/^{204}Pb$). Pb^*/Pb_c is radiogenic Pb to total common Pb (blank + initial) Th/U calculated from radiogenic $^{208}Pb/^{206}Pb$ and $^{206}Pb/^{238}U$ date; meas. is measured $^{206}Pb/^{204}Pb$ corrected for mass discrimination and tracer. Corrected atomic ratios: $^{206}Pb/^{204}Pb$ corrected for blank, mass discrimination and tracer, all others corrected for blank, mass discrimination, tracer and initial Pb, values in parentheses are 2 sigma errors in percent. Isotopic compositions of initial Pb are 18.455 ± 0.12, 15.617 ± 0.082, and 38.337 ± 0.226, based on *Stacey and Kramers* [1975] Pb evolution model. Rho is $^{206}Pb/^{238}U$ versus $^{207}Pb/^{235}U$ error correlation coefficient. Mineral dissolution and chemistry were adapted from methods developed by *Krogh* [1973], *Parrish et al.* [1987], and *Mattinson* [2005]. Five of the six grains were dissolved in steps using the CATIMS method [*Mattinson*, 2005]. Final dissolutions were spiked with a mixed $^{205}Pb/^{233}U/^{235}U$ tracer (ET535). Pb and U samples were loaded onto single rhenium filaments with silica gel and graphite, respectively; isotopic compositions were measured on a Micromass Sector 54 mass spectrometer at the University of Wyoming in either single Daly mode or multicollector, static mode with ^{204}Pb in Daly-photomultiplier collector and all other isotopes in Faraday collectors. Mass discrimination for Pb of 0.060 ± 0.06 %/amu for static Faraday runs and 0.185 ± 0.06%/amu for single Daly runs were determined by replicate analyses of NIST SRM 981. U fractionation was determined internally during each run. Procedural blanks averaged 3.2 pg Pb for zircon during the course of the study. Isotopic composition of the Pb blank was estimated as 18.719 ± 0.97, 15.662 ± 0.57, and 38.226 ± 1.42 for 206/204, 207/204, and 208/204, respectively. U blanks were consistently less than 0.2 pg. Concordia coordinates, intercepts, and uncertainties were calculated using MacPBDAT and ISOPLOT programs (based on *Ludwig* [1988, 1991]); initial Pb isotopic compositions were estimated by the *Stacey and Kramers* [1975] evolution model for 160 Ma (6/4, 7/4, 8/4: 18.455 ± 0.12, 15.617 ± 0.082, and 38.337 ± 0.226). The decay constants used by MacPBDAT are those recommended by the I.U.G.S. Subcommission on Geochronology [*Steiger and Jäger*, 1977]: 0.155125 × 10^{-9}/a for ^{238}U, 0.98485 × 10^{-9}/a for ^{235}U, and present-day $^{238}U/^{235}U$ = 137.88.

[b] The $^{206}Pb/^{238}U$ weighted mean date = 159.38 ± 0.12 Ma (0.07%) 95% confidence (MSWD = 1.8); Concordia Age = 159.45 ± 0.16 Ma 95% confidence with decay errors included.

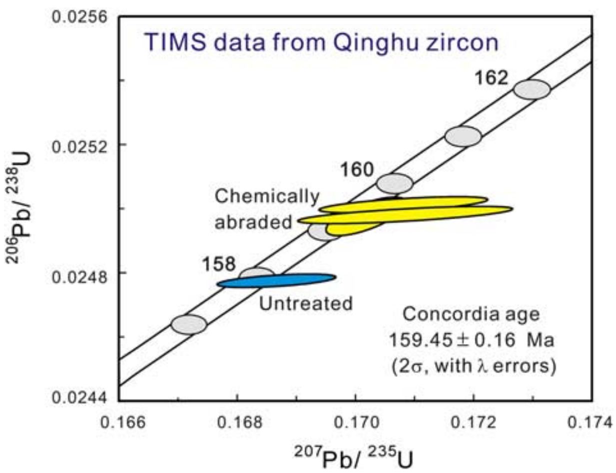

Figure 10. Conventional U-Pb Concordia diagram of ID-TIMS data from Qinghu zircon. Concordia swath depicts uncertainties due to errors in U decay constants. Yellow ellipses reflect data from five chemically abraded zircons following the method of *Mattinson* [2005]. The Concordia age is based on these data, giving the best estimate of the crystallization age. The blue ellipse represents data from an untreated, bulk dissolved grain and displays Pb loss. Data point error ellipses are 2σ.

factor of ~3 relative to the age error of 7.6% obtained by using monocollector mode.

6. Discussion and Concluding Remarks

[42] Our results presented above indicate that Paleozoic and Mesozoic zircon $^{207}Pb/^{206}Pb$ ages can be precisely and accurately dated by using multicollector SIMS without external standardization. The precision of zircon Pb/Pb age determinations depend mostly on the radiogenic Pb contents (or U contents and the age of the dated zircons). Figure 12 shows that analytical errors of the measured $^{207}Pb/^{206}Pb$ ratio (common Pb uncorrected) decrease quickly with increasing ^{207}Pb intensity between 100 and 1,000 cps, and reaches at ~0.2% with $^{207}Pb > 1,000$ cps.

[43] It is noted that the uncertainties in $^{207}Pb/^{206}Pb$ ratios measured by multicollector are very close to the expected errors from the counting statistics (Figure 12). Similarly, the uncertainties in the $^{207}Pb/^{206}Pb$ ratios measured by monocollector are also consistent with, or slightly poorer than, the expected errors from counting statistics (figure not shown). The total counting time for ^{207}Pb is 62.4 s and 240 s by monocollector and multicollector, respectively. Therefore, the counting statistics uncertainties in $^{207}Pb/^{206}Pb$ ratios by monocollector are expected to be 2 times higher than those by multicollector for the same zircon and/or baddeleyite samples (assuming constant U contents). It can be seen that the measured $^{207}Pb/^{206}Pb$ uncertainty of BR266 zircon (with fairly uniform U content) by monocollector mode is averaged at ~0.48% (Table 2), which is 2.4 times higher than the averaged uncertainty of ~0.20% by multicollector mode (Table 3). Therefore, the differences in the precision of the two techniques are mainly due to the fact that the Pb peaks are measured for 4 times longer in multicollector mode as well as elimination of the signal variation effect by simultaneous detection of Pb peaks using multicollector mode. For zircons in age of the latest Neoproterozoic to the early Paleozoic with U contents of ~1000 ppm, such as BR266 zircon, multicollector SIMS measurement is capable of achieving precisions of $^{207}Pb/^{206}Pb$ ratio of <0.1% by pooling 25 measurements, propagating an age error of <0.5% (excluding decay constant errors). For the late Paleozoic and Mesozoic (Jurassic) zircons with a few hundreds to one thousand ppm U, $^{207}Pb/^{206}Pb$ ratio can be measured with fairly good precision between 0.1% and 0.2% by pooling 25–30 measurements, propagating an age error between ~0.8% and ~3% (excluding decay constant errors). Such Pb/Pb age precision is nearly comparable with, or slightly poorer than, the $^{206}Pb/^{238}U$ age precisions obtained by conventional monocollector SIMS with external standard calibration.

[44] Our results demonstrate that the multicollector SIMS technique is suitable for determination of Pb/Pb ages of Mesozoic zircons with precisions of geological significance. This technique is therefore applicable to direct dating of zircons in thin sections without requisition of mineral separation, mounting and external standard calibration, making the microbeam U-Pb dating very efficient and petrographically significant. More importantly, it has significant implications for precise determinations of some other U-rich minerals that are not suitable for SIMS U-Pb dating by external standard calibration. For instance, baddeleyite (ZrO_2) is a very favorable mineral for dating mafic and ultramafic igneous rocks, but it is only suitable for SIMS $^{207}Pb/^{206}Pb$, rather than $^{206}Pb/^{238}U$, measurement owing to the "crystal orientation effect" that bias $^{206}Pb/^{238}U$ ratio [*Wingate and Compston*, 2000]. Zirconolite ($CaZrTi_2O_7$) also has remarkable properties for U-Pb geochronology, and could become a dominant tool for dating mafic igneous rocks [*Heaman and LeCheminant*, 1993; *Rasmussen and Fletcher*, 2004]. However, it can only be

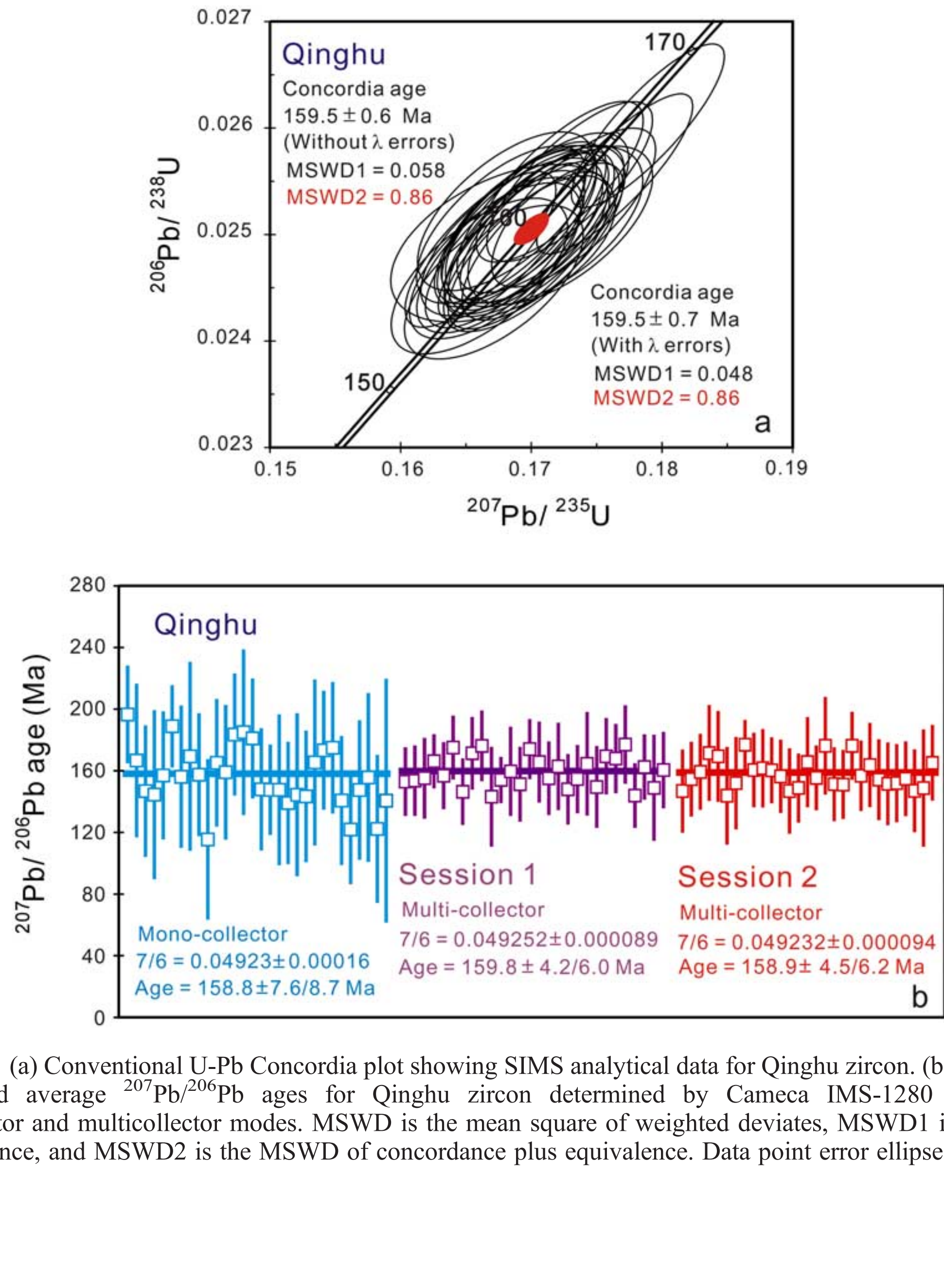

Figure 11. (a) Conventional U-Pb Concordia plot showing SIMS analytical data for Qinghu zircon. (b) Comparison of weighted average $^{207}Pb/^{206}Pb$ ages for Qinghu zircon determined by Cameca IMS-1280 SIMS using monocollector and multicollector modes. MSWD is the mean square of weighted deviates, MSWD1 is the MSWD of concordance, and MSWD2 is the MSWD of concordance plus equivalence. Data point error ellipses/bars are 2σ.

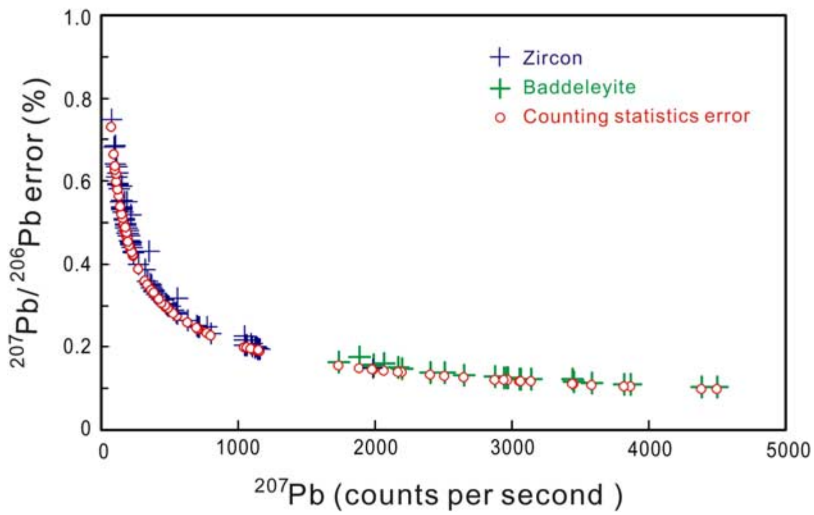

Figure 12. Correlation between the analytical error of measured $^{207}Pb/^{206}Pb$ ratio and ^{207}Pb intensity for zircon and baddeleyite. The expected uncertainties from the counting statistics, estimated as $1/(^{207}Pb \text{ intensity} \times 240 \text{ s})^{1/2}$ because ^{206}Pb intensity is about 10–20 times higher than ^{207}Pb, of each measurements are shown for comparison. It is noted that the oxygen flooding can enhance Pb^+ sensitivity by a factor exceeding 5 for baddeleyite.

precisely dated by SIMS $^{207}Pb/^{206}Pb$ measurement, because this mineral has a highly variable composition (due to extensive substitutions) that makes a matrix-matched zirconolite U-Pb age reference unavailable.

[45] The Plešovice zircon is a newly developed reference for U-Pb and Hf isotopic microbeam analysis [*Sláma et al.*, 2008]. Both LA-ICPMS and TIMS analyses give a consistent U-Pb age of 337 Ma, but the reported SIMS measurements result in a wider range of U-Pb age between 328.1 ± 4.2 Ma (1σ) and 353 ± 2.8 Ma (1σ), with a weighted mean of 341.4 ± 1.3 Ma (2σ) (excluding decay constant errors). Because of the wide age variation, the authors consider that the Plešovice zircon is not an ideal age reference material for high spatial resolution (SIMS) measurements [*Sláma et al.*, 2008]. Our SIMS measurements, however, yield very consistent U-Pb ages with the LA-ICPMS and TIMS data. It seems that the Plešovice zircon is fairly homogeneous in U-Pb age at a spatial resolution of ~20–30 μm, and can be used as a good U-Pb zircon age reference for SIMS measurement. We noted that *Sláma et al.* [2008] used a smaller primary ion beam of ~15 μm than our measurements, and further examinations of homogeneity in U-Pb age at a spatial resolution <20 μm are likely needed.

Acknowledgments

[46] We thank H. Tao for mounting zircon and baddeleyite samples and H. Zhou for documentation of micrographs and cathodoluminescence images. George Gehrels, Ian Williams, and Sandra Kamo provided careful and constructive reviews that significantly improved the manuscript. This work was supported by the National Natural Science Foundation of China (grants 40773007 and 40873045) and the Institute of Geology and Geophysics, Chinese Academy of Sciences (grant ZC0801).

References

Bosch, D., D. Hammor, O. Bruguier, R. Caby, and J.-M. Luck (2002), Monanite "in situ" 207Pb/206Pb geochronology using a small geometry high-resolution ion probe. Application to Archaean and Proterozoic rocks, *Chem. Geol.*, *184*, 151–165, doi:10.1016/S0009-2541(01)00361-8.

Compston, W. (1999), Geological age by instrumental analysis: The 29th Hallimond Lecture, *Mineral. Mag.*, *63*, 297–311, doi:10.1180/002646199548475.

Compston, W., I. S. Williams, and C. Meyer (1984), U-Pb geochronology of zircons from lunar breccia 73217 using a sensitive high mass-resolution ion microprobe, *J. Geophys. Res.*, *89*(S2), B525–B534, doi:10.1029/JB089iS02p0B525.

Davis, D. W., I. S. Williams, and T. E. Krogh (2003), Historical development of zircon geochronology, *Rev. Mineral. Geochem.*, *53*, 145–181, doi:10.2113/0530145.

Heaman, L. M. (2009), The application of U–Pb geochronology to mafic, ultramafic and alkaline rocks: An evaluation of three mineral standards, *Chem. Geol.*, *261*, 42–51, doi:10.1016/j.chemgeo.2008.10.021, in press.

Heaman, L. M., and A. N. LeCheminant (1993), Paragenesis and U-Pb systematics of baddeleyite (ZrO_2), *Chem. Geol.*, *110*, 95–126, doi:10.1016/0009-2541(93)90249-I.

Ireland, T. R., and I. S. Williams (2003), Considerations in zircon geochronology by SIMS, in *Zircon*, edited by J. M. Hanchar and P. W. O. Hoskin, *Rev. Mineral. Geochem.*, *53*, 215–241.

Jaffey, A. H., K. F. Flynn, L. E. Glendenin, W. C. Bentley, and A. M. Essling (1971), Precision measurement of half-lives and specific activities of ^{235}U and ^{238}U, *Phys. Rev. C*, *4*, 1889–1906, doi:10.1103/PhysRevC.4.1889.

Košler, J., and P. J. Sylvester (2003), Present trends and the future of zircon in geochronology: Laser ablation ICPMS, in *Zircon*, edited by J. M. Hanchar and P. W. O. Hoskin, *Rev. Mineral. Geochem.*, *53*, 243–275.

Krogh, T. E. (1973), A low-contamination method for hydrothermal decomposition of zircon and extraction of U and Pb for isotopic age determinations, *Geochim. Cosmochim. Acta*, *37*, 485–494, doi:10.1016/0016-7037(73)90213-5.

Li, X. H., X. Liang, M. Sun, H. Guan, and J. G. Malpas (2001), Precise $^{206}Pb/^{238}U$ age determination on zircons by laser ablation microprobe-inductively coupled plasma-mass spectrometry using continuous linear ablation, *Chem. Geol.*, *175*, 209–219, doi:10.1016/S0009-2541(00)00394-6.

Li, X. H., S. L. Chung, H. W. Zhou, C. H. Lo, Y. Liu, and C. H. Chen (2004), Jurassic intraplate magmatism in southern Hunan-eastern Guangxi: $^{40}Ar/^{39}Ar$ dating, geochemistry, Sr-Nd isotopes and implications for tectonic evolution of SE China, in *Aspects of the Tectonic Evolution of China*, edited by J. Malpas et al., *Geol. Soc. Spec. Publ.*, *226*, 193–216.

Li, X. H., L. Su, S. L. Chung, Z. X. Li, Y. Liu, B. Song, and D. Y. Liu (2005), Formation of the Jinchuan ultramafic intrusion and the world's third largest Ni-Cu sulfide deposit: Associated with the ∼825 Ma south China mantle plume?, *Geochem. Geophys. Geosyst.*, *6*, Q11004, doi:10.1029/2005GC001006.

Ludwig, K. R. (1980), Calculation of uncertainties of U-Pb isotope data, *Earth Planet. Sci. Lett.*, *46*, 212–220, doi:10.1016/0012-821X(80)90007-2.

Ludwig, K. R. (1988), PBDAT for MS-DOS, a computer program for IBM-PC compatibles for processing raw Pb-U-Th isotope data, version 1.24, *U.S. Geol. Surv. Open File Rep.*, *88-542*, 32 pp.

Ludwig, K. R. (1991), ISOPLOT for MS-DOS, a plotting and regression program for radiogenic-isotope data, for IBM-PC compatible computers, version 2.75, *U.S. Geol. Surv. Open File Rep.*, *91-445*, 45 pp.

Ludwig, K. R. (1998), On the treatment of concordant uranium-lead ages, *Geochim. Cosmochim. Acta*, *62*, 665–676, doi:10.1016/S0016-7037(98)00059-3.

Ludwig, K. R. (2001), Users manual for Isoplot/Ex rev. 2.49, *Spec. Publ. 1a*, Berkeley Geochronol. Cent., Berkeley, Calif.

Mattinson, J. M. (2005), Zircon U-Pb chemical abrasion (''CA-TIMS'') method: Combined annealing and multi-step partial dissolution analysis for improved precision and accuracy of zircon ages, *Chem. Geol.*, *220*, 47–66, doi:10.1016/j.chemgeo.2005.03.011.

Parrish, R. R., J. C. Roddick, W. D. Loveridge, and R. D. Sullivan (1987), Uranium-lead analytical techniques at the geochronology laboratory, Geological Survey of Canada, in *Radiogenic Age and Isotopic Studies*, *Pap. Geol. Surv. Can.*, *87-2*, 3–7.

Quidelleur, X., M. Grove, O. M. Lovera, T. M. Harrison, A. Yin, and F. J. Ryerson (1997), The thermal evolution and slip history of the Renbu Zedong Thrust, southeastern Tibet, *J. Geophys. Res.*, *102*, 2659–2679.

Rasmussen, B., and I. R. Fletcher (2004), Zirconolite: A new U-Pb chronometer for mafic igneous rocks, *Geology*, *32*, 785–788, doi:10.1130/G20658.1.

Schoene, B., J. L. Crowley, D. J. Condon, M. D. Schmitz, and S. A. Bowring (2006), Reassessing the uranium decay constants for geochronology using ID-TIMS U-Pb data, *Geochim. Cosmochim. Acta*, *70*, 426–445, doi:10.1016/j.gca.2005.09.007.

Schuhmacher, M., E. de Chambost, K. D. McKeegan, T. M. Harrison, and H. Migeon (1994), In situ dating of zircon with the Cameca IMS 1270, in *Secondary Ion Mass Spectrometry SIMS IX*, edited by A. Benninghoven, B. Hagenhoff, and H. W. Werner, pp. 919–922, John Wiley, Chichester, U. K.

Sláma, J., et al. (2008), Plešovice zircon—A new natural reference material for U–Pb and Hf isotopic microanalysis, *Chem. Geol.*, *249*, 1–35, doi:10.1016/j.chemgeo.2007.11.005.

Stacey, J. S., and J. D. Kramers (1975), Approximation of terrestrial lead isotope evolution by a two-stage model, *Earth Planet. Sci. Lett.*, *26*, 207–221.

Steiger, R. H., and E. Jäger (1977), Subcommission on geochronology: Convention on the use of decay constants in geo- and cosmochronology, *Earth Planet. Sci. Lett.*, *36*, 359–362, doi:10.1016/0012-821X(77)90060-7.

Stern, R. A. (2001), A new isotopic and trace-element standard for the ion microprobe: Preliminary thermal ionisation mass spectrometry (TIMS) U-Pb and electron-microprobe data, *Curr. Res. 2001-F*, Geol. Surv. of Can., Ottawa, Ont., Canada.

Stern, R. A., and Y. Amelin (2003), Assessment of errors in SIMS zircon U-Pb geochronology using a natural zircon standard and NIST SRM 610 glass, *Chem. Geol.*, *197*, 111–142, doi:10.1016/S0009-2541(02)00320-0.

Whitehouse, M. J., S. Claesson, T. Sunde, and J. Vestin (1997), Ion-microprobe U-Pb zircon geochronology and correlation of Archaean gneisses from the Lewisian Complex of Gruinard Bay, north-west Scotland, *Geochim. Cosmochim. Acta*, *61*, 4429–4438, doi:10.1016/S0016-7037(97)00251-2.

Whitehouse, M. J., B. S. Kamber, and S. Moorbath (1999), Age significance of U-Th-Pb zircon data from early Archaean rocks of west Greenland—A reassessment based on combined ion-microprobe and imaging studies, *Chem. Geol.*, *160*, 201–224, doi:10.1016/S0009-2541(99)00066-2.

Wiedenbeck, M., P. Alle, F. Corfu, W. L. Griffin, M. Meier, F. Oberli, A. Vonquadt, J. C. Roddick, and W. Speigel (1995), Three natural zircon standards for U-Th-Pb, Lu-Hf, trace-element and REE analyses, *Geostand. Newsl.*, *19*, 1–23, doi:10.1111/j.1751-908X.1995.tb00147.x.

Wiedenbeck, M., et al. (2004), Further characterisation of the 91500 zircon crystal, *Geostand. Geoanal. Res.*, *28*, 9–39, doi:10.1111/j.1751-908X.2004.tb01041.x.

Wingate, M. T. D., and W. Compston (2000), Crystal orientation effects during ion microprobe U-Pb analysis of baddeleyite, *Chem. Geol.*, *168*, 75–97, doi:10.1016/S0009-2541(00)00184-4.

Wingate, M. T. D., and J. W. Giddings (2000), Age and palaeomagnetism of the Mundine Well dyke swarm, Western Australia: Implications for an Australia-Laurentia connection at 755 Ma, *Precambrian Res.*, *100*, 335–357, doi:10.1016/S0301-9268(99)00080-7.

Yuan, H. L., S. Gao, M. N. Dai, C. L. Zong, D. Günther, G. H. Fontaine, X. M. Liu, and C. R. Diwu (2008), Simultaneous determinations of U-Pb age, Hf isotopes and trace element compositions of zircon by excimer laser-ablation quadrupole and multiple-collector ICP-MS, *Chem. Geol.*, *247*, 100–118, doi:10.1016/j.chemgeo.2007.10.003.